

Université de Montréal

A test of articular modelling in response to load in human upper limbs

Par
Karyne Rabey

Département d'Anthropologie
Faculté des Arts et Sciences

Mémoire présenté à la faculté des études supérieures
En vue d'obtention du grade de M.Sc. en Anthropologie

Décembre, 2006

© Karyne Rabey, 2006



GW
H
U54
2007
V.019

AVIS

L'auteur a autorisé l'Université de Montréal à reproduire et diffuser, en totalité ou en partie, par quelque moyen que ce soit et sur quelque support que ce soit, et exclusivement à des fins non lucratives d'enseignement et de recherche, des copies de ce mémoire ou de cette thèse.

L'auteur et les coauteurs le cas échéant conservent la propriété du droit d'auteur et des droits moraux qui protègent ce document. Ni la thèse ou le mémoire, ni des extraits substantiels de ce document, ne doivent être imprimés ou autrement reproduits sans l'autorisation de l'auteur.

Afin de se conformer à la Loi canadienne sur la protection des renseignements personnels, quelques formulaires secondaires, coordonnées ou signatures intégrées au texte ont pu être enlevés de ce document. Bien que cela ait pu affecter la pagination, il n'y a aucun contenu manquant.

NOTICE

The author of this thesis or dissertation has granted a nonexclusive license allowing Université de Montréal to reproduce and publish the document, in part or in whole, and in any format, solely for noncommercial educational and research purposes.

The author and co-authors if applicable retain copyright ownership and moral rights in this document. Neither the whole thesis or dissertation, nor substantial extracts from it, may be printed or otherwise reproduced without the author's permission.

In compliance with the Canadian Privacy Act some supporting forms, contact information or signatures may have been removed from the document. While this may affect the document page count, it does not represent any loss of content from the document.

Université de Montréal
Faculté des études supérieures

Ce mémoire intitulé:

A test of articular modelling in response to load in human upper limbs

Présenté par:

Karyne Rabey

a été évalué par un jury composé des personnes suivantes:

Isabelle Ribot
président-rapporteur

Michelle Drapeau
directeur de recherche

Bernard Chapais
membre du jury

Abstract

It has long been recognized that mechanical loading plays an important role in skeletal development. Articulations were often considered to be less responsive to the mechanical environment and be much more constraint genetically than the long bone diaphysis. However, recent animal studies have shown that mechanical loads do influence joint architecture. Still, the contribution of the mechanical environment during bone growth to the variability of joint surface size and shape is incompletely understood, particularly in humans. This project tests the hypothesis that joint surfaces are, in part, shaped by the mechanical environment. Most humans use preferably one arm over the other and as a result, have stronger muscles on the preferred side. Specifically, this project tests the hypothesis that the side that has larger muscle markings will have joints that are modelled to accommodate larger loads by being larger or shaped differently. Least-square regression was used to evaluate the influence of muscle size on the upper-limb articulations' shape and size on a sample of 108 humans from pre-industrialized populations. Results show that, unlike what was expected upper-limb articulations are rarely asymmetrical relative to muscular asymmetry. Only a few left-right comparisons support the hypothesis that the side with larger muscle markings will have joints that are larger or shaped differently. These unexpected results suggests that right-left differences in the articulations may be very small or the sample too small to observe any significant differences in the upper-limb articular morphology.

Key words: Anthropology, biology, growth, articulation, muscle insertions.

Résumé

Il est reconnu depuis longtemps que les charges mécaniques jouent un rôle important sur le développement osseux. Les articulations ont souvent été considérées moins malléables à l'environnement mécanique et plus contraintes génétiquement que les diaphyses des os longs. Cependant, des études récentes sur des animaux ont démontré que les charges mécaniques ont une influence sur l'architecture des articulations. Malgré ceci, la contribution de l'environnement mécanique durant le développement osseux à la variabilité de la taille et de la forme des surfaces articulaires n'est pas complètement comprise, surtout chez les humains. Ce projet teste l'hypothèse selon laquelle les surfaces articulaires sont en partie formées par l'environnement mécanique. La plupart des humains utilisent préférentiellement un bras plutôt que l'autre et ont donc des muscles plus forts sur le côté le plus utilisé. De façon plus spécifique, ce projet teste l'hypothèse selon laquelle le côté ayant de plus grandes insertions musculaires aura des articulations qui seront modelées pour accommoder les plus grandes charges, en étant soit de taille ou de forme différente. Des régressions linéaires sur un échantillon de 108 humains de populations préindustrielles ont été utilisées afin d'évaluer l'influence de la taille des insertions musculaires sur la taille et la forme des articulations du membre supérieur. Contrairement à ce qui était attendu, les résultats montrent que les articulations du membre supérieur sont rarement asymétriques relativement à l'asymétrie musculaire. Seulement quelques comparaisons droite-gauche supportent l'hypothèse que le côté avec les plus grandes insertions musculaires aura des articulations de taille et/ou de forme différente. Ces résultats inattendus suggèrent que les différences droite-gauche dans les articulations sont peut-être très faibles ou que l'échantillon est trop petit pour pouvoir observer des différences significatives dans la morphologie des articulations du membre supérieur.

Mots clés : Anthropologie, biologie, développement, articulations, insertions musculaires.

Table of contents

Abstract	iii
Résumé	iv
Table of contents	v
List of figures	vi
List of tables	viii
Acknowledgements	x
Chapter 1: Introduction	1
1.1 Introduction.....	1
1.2 Chondral modelling theory	2
1.3 Mechanotransduction	5
1.4 Muscle attachments.....	8
1.5 Hypotheses to be tested.....	10
Chapter 2: Materials and methods	16
2.1 Materials.....	16
2.2 Methods.....	17
2.3 Analysis.....	23
Chapter 3: Results	25
3.1 Shoulder; size.....	25
3.2 Elbow; size.....	26
3.3 Wrist; size.....	31
3.4 Hand; size.....	32
3.5 Shoulder; shape	32
3.6 Elbow; shape	33
3.7 Wrist; shape.....	36
3.8 Hand; shape.....	37
3.9 Summary	38
Chapter 4: Discussion and conclusion	40
4.1 General discussion	40
4.2 Shoulder	40
4.3 Elbow	41
4.3.1 <i>Distal humerus</i>	42
4.3.2 <i>Proximal ulna and radius</i>	43
4.4 Wrist.....	45
4.5 Conclusion	45
Bibliography	49

List of figures

Figure I: Representation of adjoining joint surfaces to demonstrate the problems of incongruence and lack of smoothness. A raised area, indicated by the arrow, concentrates the load over a small portion of the joint surface. To increase congruence and smoothness and reduce large loads per unit, the growth will stop where there is high stress (raised area). Where there is little stress in areas around the raised surface, growth will be stimulated. This will alter the joint curvature and maintain a normal kinematic pathway (from Plochocki, 2003). ...4

Figure II: How mechanical use and disuse may regulate bone modelling. Normal mechanical use would maintain levels of osteoblast and osteoclast activation. Increased fluid flow in lacunae and canaliculi from overuse will increase osteocyte stress levels and osteoblast activation. Lower levels of fluid flow from disuse increase osteoclast activation and/or decrease activation of osteoclast suppressors (from Plochocki, 2003).7

Figure III: Muscle attachment sites of the upper limbs (from Nordin and Frankel, 2001).9

Figure IV: Example of muscle contraction shown by the *deltoideus* (above-left) and the *pectoralis major* (below-right) on the shoulder joint causing the head of the humerus to compress the glenoid surface of the scapula. The black arrow represents the medially directed load from the muscular contraction acting on the shoulder articulation. Figure shows anterior view of the shoulder (from Sénécal, 2003).12

Figure V: Example of the muscle contractions caused by the flexors and extensors of the forearm acting on the elbow articulation (from Platzner, 2001). Figures show anterior views of the elbow.13

Figure VI: Schematic illustration showing a strong medial keel on the elbow articulation (from Schmitt, 2003).13

Figure VII: Pronation (rotation of the hand laterally) and supination (rotation of the hand medially) movements of the forearm (from DePuy Orthopaedics, 2005).14

Figure VIII: Points taken on the shoulder, lateral view. The superior (1), middle (5) and inferior (3) points form the SI angle and the anterior (2), middle (5) and posterior (4) points form the AP angle.19

Figure IX: Points taken and angles calculated at the humero-ulnar articulation, anterior view. A - Inferior medial angle (points 1, 3, 2), B - Inferior lateral angle (points 1, 3, 4), and C - Medial angle of the humeral trochlea (points 2, 3, 4).19

Figure X: Points taken at proximal surface of the radius, superior view. The medial (2), middle (5) and lateral (4) points form the ML angle and the anterior (1), middle (5) and posterior (3) points form the AP angle.	20
Figure XI: Points taken at the distal surface of the radius, inferior view. Anteriorly the medial (3), middle (6) and lateral (1) points form the ML angle 1 and ML angle 2 is posteriorly (1, 6, 4). The anterior (2), middle (6) and posterior (5) points form the AP angle.....	20
Figure XII: Points taken at the proximal surface of the first metacarpal, superior view. The medial (2), middle (5) and lateral (4) points form the ML angle and the anterior (1), middle (5) and posterior (3) points form the AP angle.	21
Figure XIII: Regression between size of the humeral head and the size of the greater tubercle.....	26
Figure XIV : Regression between the size of the SI height of the capitulum and the size of the lateral epicondyle.....	27
Figure XV: Regression of the size of the SI height of the capitulum and the size of the insertion of the <i>pronator teres</i> muscle.....	28
Figure XVI: Regression between the size of the trochlea and the size of the olecranon.....	28
Figure XVII: Regression between the size of the radial head and the size of the radial tuberosity.....	30
Figure XVIII: Regression between the size of the radial notch and the size of the insertion of the <i>supinator</i> muscle.....	31
Figure XIX: Regression of the shape values of the inferior lateral angle (B) of the humeral trochlea and ulnar tuberosity.....	34
Figure XX: Regression of the shape values of the inferior lateral angle of the humeral trochlea (B) and the radial tuberosity.....	34
Figure XXI: Regression of the shape values of the AP angle of the radial head and the olecranon.	36
Figure XXII: Regression of the shape values of the ML angle 2 of the distal radius and the insertion of the <i>abductor pollicis longus</i> muscle.....	37

List of tables

Table 1: Study sample.....	16
Table 2: Linear measurements	17
Table 3: Muscle attachments.....	21
Table 4: Measurement errors for the articular measurements of the left and right sides included in this study (n = 3 individuals).....	22
Table 5: Measurement errors for the muscle site measurements of the right and left sides included in this study (n = 3 individuals).	23
Table 6: Correlation coefficients and significance of the regressions of articular size and muscle attachment size at the shoulder	25
Table 7: Correlation coefficients and significance of the regressions of articular size and muscle attachment size at the distal humerus	27
Table 8: Correlation coefficients and significance of the regressions of articular size and muscle attachment size at the proximal ulnar measurements	29
Table 9: Correlation coefficients and significance of the regressions of articular size and muscle attachment size at the proximal ulna and radius	30
Table 10: Correlation coefficients and significance of the regressions of articular size and muscle attachment size at the wrist.....	31
Table 11: Correlation coefficients and significance of the regressions of articular size and muscle attachment size at the hand.....	32
Table 12: Correlation coefficients and significance of the regressions of articular shape and muscle attachment size at the glenoid cavity	32
Table 13: Correlation coefficients and significance of the regressions of articular shape and muscle attachment size at the distal humerus	33
Table 14: Correlation coefficients and significance of the regressions of articular shape and muscle attachment size at the radial head	35
Table 15: Correlation coefficients and significance of the regressions of articular shape and muscle attachment size at the distal radius	36
Table 16: Correlation coefficients and significance of the regressions of articular shape and muscle attachment size at the hand.....	37

Table 17: Summary of the results from the regressions where $p \leq 0.1$ and $r \geq 0.20$	39
--	----

Acknowledgements

I would like to thank my supervisor Dr. Michelle Drapeau for all the time and encouragement she has given me the past two years. I am very grateful of all the comments, critiques, reflections and discussions we shared. I learned so much under her supervision, it was a great experience.

Thanks are also due to Dr. Jerome Cybulski, Janet Young and Stacey Girling-Christie from the Canadian Museum of Civilization for the help and support they gave me while I was working on the collection in their care. Special thank goes to Dr. Jerome Cybulski for all the extra time he took to assure I had everything I needed during my stay at the museum. I also want to thank the Inuit Trust Heritage for granting me permission to study the priceless Nunavut collection.

I would also like to express my gratitude to my parents, Lise and Robert, and my brother Alan for keeping up with me all these years. All of my family, Gaëtane, Aldo, Maxime, Marc, Marika and Jocelyne, you've encouraged me to go all the way and to keep doing what I love no matter what. Each and every one of you has participated in your own way in my journey! Special thanks go to William and Linda for giving me shelter while I visited the museum.

A big thank you also goes to all my friends who have helped and supported me through the good and the tough times. Marie-Eve, Claudiane, Sabrina, Constance, Catherine, Sadia; you guys have been there from the beginning, and to all of you that came about in the last year at the lab; Marie-Christine and Claude, you have been wonderful in your time and encouragements. I can not forget all those friends that are not at the University but have also contributed in keeping me sane, you guys know who you are! And a special thank you to "Dude" for being the best person in the world and keeping up with me.

Last, but certainly not least, I would like to thank Dr. Bernard Chapais and Dr. Isabelle Ribot for the comments and critiques you have given me on my research and future decisions.

Chapter 1: Introduction

1.1 Introduction

It is recognized that mechanical loading plays an important role in skeletal development (Martin et al., 1998; Frost, 1999; Hamrick, 1999, 2000; Carter and Beaupré, 2001; Lieberman et al., 2001; Nordin and Frankel, 2001; Plochocki, 2004, 2006). Bone is a dynamic tissue in constant modification, so it is often modelled by the activities practiced by an individual. Given this plasticity, bone is an invaluable tool for the study of evolution, human behaviour, etc. For years, many researchers have concentrated their efforts on the cross section of the bones to understand bone modelling and remodelling, because it has long been accepted that during growth, cross section of the diaphyses responds well to mechanical loads. Long bone diaphyses grow thicker and stronger as bone length, body mass and loading increase (Ruff et al., 1994; Carter and Beaupré, 2001; Pearson and Lieberman, 2004). Since long bones modify their shape to better resist bending, twisting and compressions, then the cross-sectional geometry of an animal's bones is a good indicator of the mechanical forces induced to the animal and thus a reasonable reflection of habitual activities (Ruff, 2002a). On the other hand, articulations were often considered to be less responsive to the mechanical environment and be much more constraint genetically (Lieberman et al., 2001).

However, recent animal studies (Frost, 1999; Hamrick, 1999a, b; Carter and Beaupré, 2001; Plochocki, 2006) have shown that mechanical loads do influence joint architecture. Frost (1999) observed that compared to congenitally or neonatally paralyzed limbs, joints in normal limbs develop greater diameters, greater radii of curvature and surface area, thicker capsules and ligaments and more subchondral bone to support their articular cartilage. Those differences reveal the effects of postnatal mechanical usage on a growing joint's design and biologic activities. Plochocki (2006) found that exercise-induced mechanical loading affected the size, shape, and the distribution of joint tissue. He concluded that the mechanical regulation of articular

proliferation allows for continual adaptation of joint form. Larger, flatter subchondral surfaces and greater chondral and osseous tissue areas appear to take *in vivo* adaptations that provide greater resistance against larger loads. Shape of the articular surface is therefore shown to be modified during growth in response to loads, including those incurred by muscular contractions, in order to reduce the risk of damage to the articular cartilage (Frost, 1999; Hamrick, 1999b; Carter and Beaupré, 2001; Plochocki, 2006). Still, few studies (e.g., Tankakura et al., 1986) have demonstrated joint plasticity in humans. The contribution of the mechanical environment during bone growth to the variability of joint surface size and shape is still incompletely understood.

This project tests the hypothesis that joint surfaces are, in part, shaped by the mechanical environment. It tests whether individuals with larger muscle markings are characterized by differently shaped joints or proportionally larger joints. Most humans use preferably one arm over the other and as a result, have stronger muscles on the preferred side. Specifically, this project will test the hypothesis that the side that has larger muscle markings will have joints that are modelled to accommodate larger loads. For each individual, the joint should be larger and/or of a shape that better resist loads on the preferred side when compared to the other side. The analysis of joint form and size is a key component to anthropological investigations such as the biomechanics of bones and articular shape in evolutionary and prehistoric contexts. A thorough understanding of the determinants that shape joints is essential for accurately interpreting the biology, behaviour, and evolutionary history of humans (Plochocki, 2003). It is therefore necessary to better understand the relationship between joint form and the mechanical environment.

1.2 Chondral modelling theory

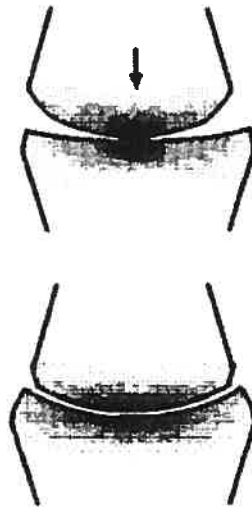
Carter and Beaupré (2001) explain how muscular movements on the skeleton are essential to have the desired structure of the articular surfaces right from the beginning of ontogeny. The absence of muscular activity in the developing chick embryo has been shown to cause distortion of skeletal rudiments, absence of joint cavities and fusion (fibrous, cartilaginous, or

osseous) across the joint regions. Tensile forces from muscles must create high stresses in the interzones (sites of future bone articulations). This will eventually lead to cleavage, joint motion and cavitations. Movement at the joint therefore, helps to control and guide the contour of the joint surface so that it develops a kinematically efficient shape (Frost, 1999; Hamrick, 1999a, b; Carter and Beaupré, 2001). Mechanical loading associated with the postnatal development of posture and locomotion may provide an important stimulus for the progression of ossification and the formation of articular cartilage in the epiphyses of growing mammals. Frost (1994, 1999), then Hamrick (1999b) looked at the process by which, after formation of the joint cavities, limb joints maintain congruence.

The chondral modelling theory (Frost, 1994, 1999; Hamrick, 1999b) tries to explain the relationship between mechanical environment and joint form. The theory proposes that the mechanical loadings to which limb joints are subjected during growth affect cartilage proliferation at the articular surface, which strongly influences adult joint conformation. The theory argues that joint size, shape and congruence are maintained throughout mammalian postnatal ontogeny, in part, by the regulation of cartilage growth in articular regions by mechanical stress. Chondral modelling serves as a physiological mechanism that maintains a normal kinematic pathway through joints while preventing excessive loads that could irreparably damage articular cartilage (Frost, 1994, 1999; Hamrick, 1999b; Plochocki, 2003).

Frost's (1994, 1999) theory proposes that cartilage growth will cease in a region bearing excessive compressive load and increase in adjacent less loaded regions (Figure I). The direction of the cartilage growth and alignment of cartilage layers will always reflect the magnitude and direction of prevailing loads at the articular surface.

Figure I: Representation of adjoining joint surfaces to demonstrate the problems of incongruence and lack of smoothness. A raised area, indicated by the arrow, concentrates the load over a small portion of the joint surface. To increase congruence and smoothness and reduce large loads per unit, the growth will stop where there is high stress (raised area). Where there is little stress in areas around the raised surface, growth will be stimulated. This will alter the joint curvature and maintain a normal kinematic pathway (from Plochocki, 2003).



It is the relative magnitude, frequency, and distribution of hydrostatic pressure that regulate the metabolic activity of chondrocytes and not compressive loading per se. Frost's theory is non-specific regarding the role of particular tissue layers in the modelling process and provides few specific details as to how mechanotransduction might regulate articular cartilage growth and development (Hamrick, 1999b).

Hamrick (1999b) expanded on Frost's original theory and explained further the mechanisms that facilitate functional integration in the developing mammalian locomotor system. The chondral modelling theory makes predictions based on the premise that hydrostatic compressive stress from the mechanical loading of cartilage affects local bone growth at the articular surface through the transduction of mechanical energy. The response will vary as stress, magnitudes, frequencies, and orientations vary throughout ontogeny.

The predictions of the theory are:

- (1) Peak levels of hydrostatic pressures in articular cartilage increase between birth and skeletal maturity because articular cartilage thickness decreases, force generation increases, and relative joint size decreases.
- (2) The articular cartilage of growing mammals responds to this ontogenetic increase in joint stress by a process of chondral modelling: chondrocyte (mature chondroblast cell) division and cartilage matrix synthesis in response to changes in tissue's mechanical environment.
- (3) Hydrostatic pressure at a certain range and frequency stimulates chondrocyte division and matrix synthesis. The importance of load frequency and periodicity in stimulating bone modelling and remodelling is emphasized.
- (4) Chondrocyte metabolism can also be inhibited by loads that are static, infrequent, weak, or excessive.

Evidence from *in vitro* and *in vivo* studies suggests that mechanotransduction is an important determinant of articulation growth and form. The regulation of cartilage growth by mechanical load is a primary mechanism by which extrinsic factors influence limb joint morphogenesis. While mechanotransduction (see below) explains the cellular physiological effects of mechanical stress on chondrocyte maturation, the chondral modelling theory explains the relationship between gross joint design and joint function throughout postnatal skeletal growth. This makes an understanding of chondral modelling useful for interpreting the significance of joint shape variation and understanding the evolutionary history, prehistory and adaptations of humans and other species (Plochocki, 2003)

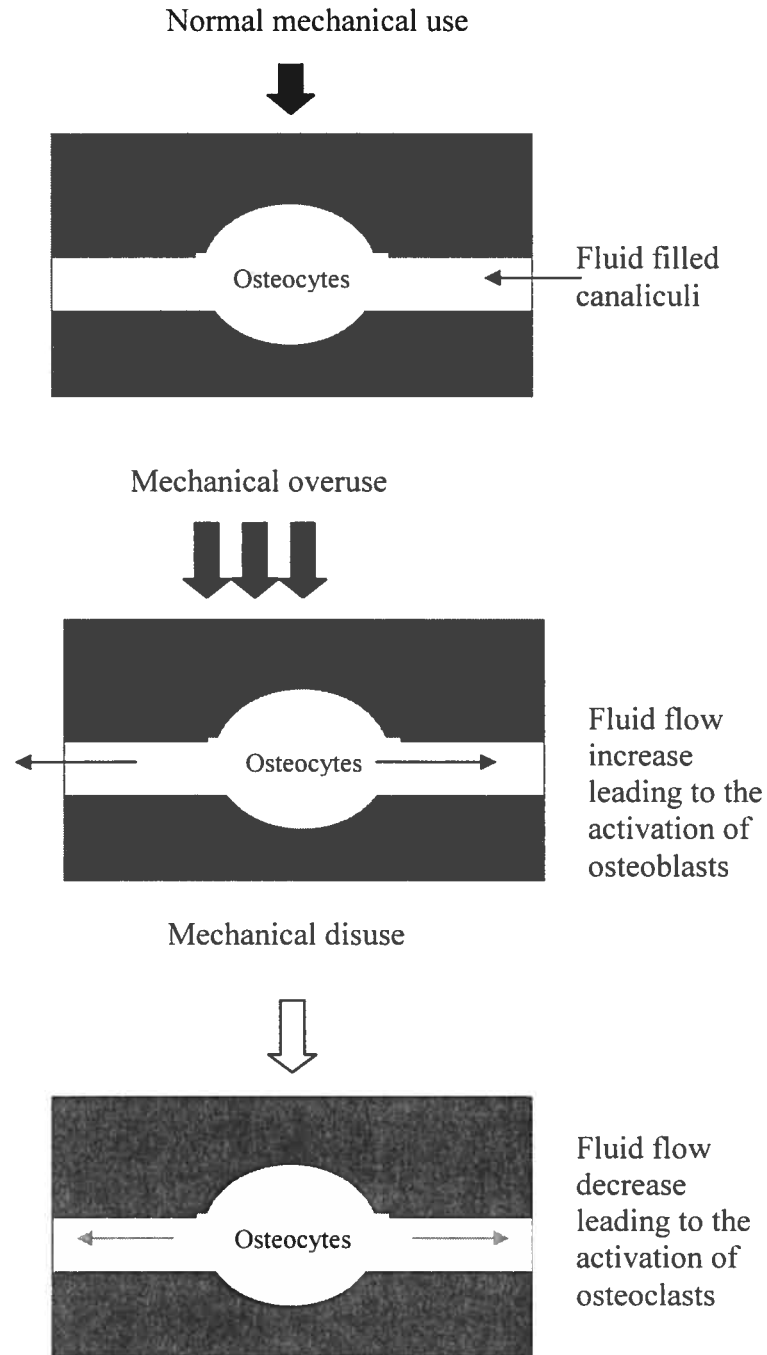
1.3 Mechanotransduction

Mechanotransduction is the biological process of converting mechanical energy into electrical and biomechanical signals and by which the physiological adaptation of bone and cartilage to the mechanical environment occurs. These

are still not fully understood today, but a brief description of the state of knowledge follows. Osteocytes (mature bone cells) act as mechano-sensors (cells that sense applied mechanical loadings). Osteocytes lie in fluid-filled cavities (lacunae) in bones and extend processes outward through canaliculi (small channels). When bone is loaded, the direct deformation of bone cells is extremely small. However, interstitial fluid flow in the canals exerts fluid shear stresses on the osteocyte surface sufficient to kick off a biomechanical response (Figure II). Osteocytes seem to be sensitive to pressure from fluids in the lacunae and canaliculi and express genes for bio-signals that affect osteoblasts (bone-forming cells responsible for synthesizing and depositing bone material often concentrated beneath the periosteum) and osteoclast (cells responsible for the resorption or removal of bone tissue) activity. Mechanically loaded, these bone cells express mRNA for insulin growth factor-1 (IGF-1) that promote bone formation and stimulates osteoclast and osteoblast differentiation. As a result, mechanical stresses affecting osteocytes trigger the process of bone modelling and remodelling. Osteoclasts and osteoblasts are activated and then alter the internal structure of bone in response to mechanical loading by locally resorbing and depositing bone. Through this physiological mechanism, bone can adapt to the mechanical environment.

In cartilage, chondrocytes act as mechano-sensors. They alter their biological activity in response to mechanical, osmotic and fluid stress. The complete process of the transduction of mechanical stress in cartilage is not well understood due to complex properties of the constituents in the extracellular matrix. However, it seems that osmotic pressure provides the mechano-electrochemical stimuli that initiates the physiological response and alters chondrocytes metabolic activity. Chondrocytes are responsible for bone growth and produce extracellular matrix that gives cartilage its mechanical properties (Plochocki, 2003).

Figure II: How mechanical use and disuse may regulate bone modelling. Normal mechanical use would maintain levels of osteoblast and osteoclast activation. Increased fluid flow in lacunae and canaliculi from overuse will increase osteocyte stress levels and osteoblast activation. Lower levels of fluid flow from disuse increase osteoclast activation and/or decrease activation of osteoclast suppressors (from Plochocki, 2003).



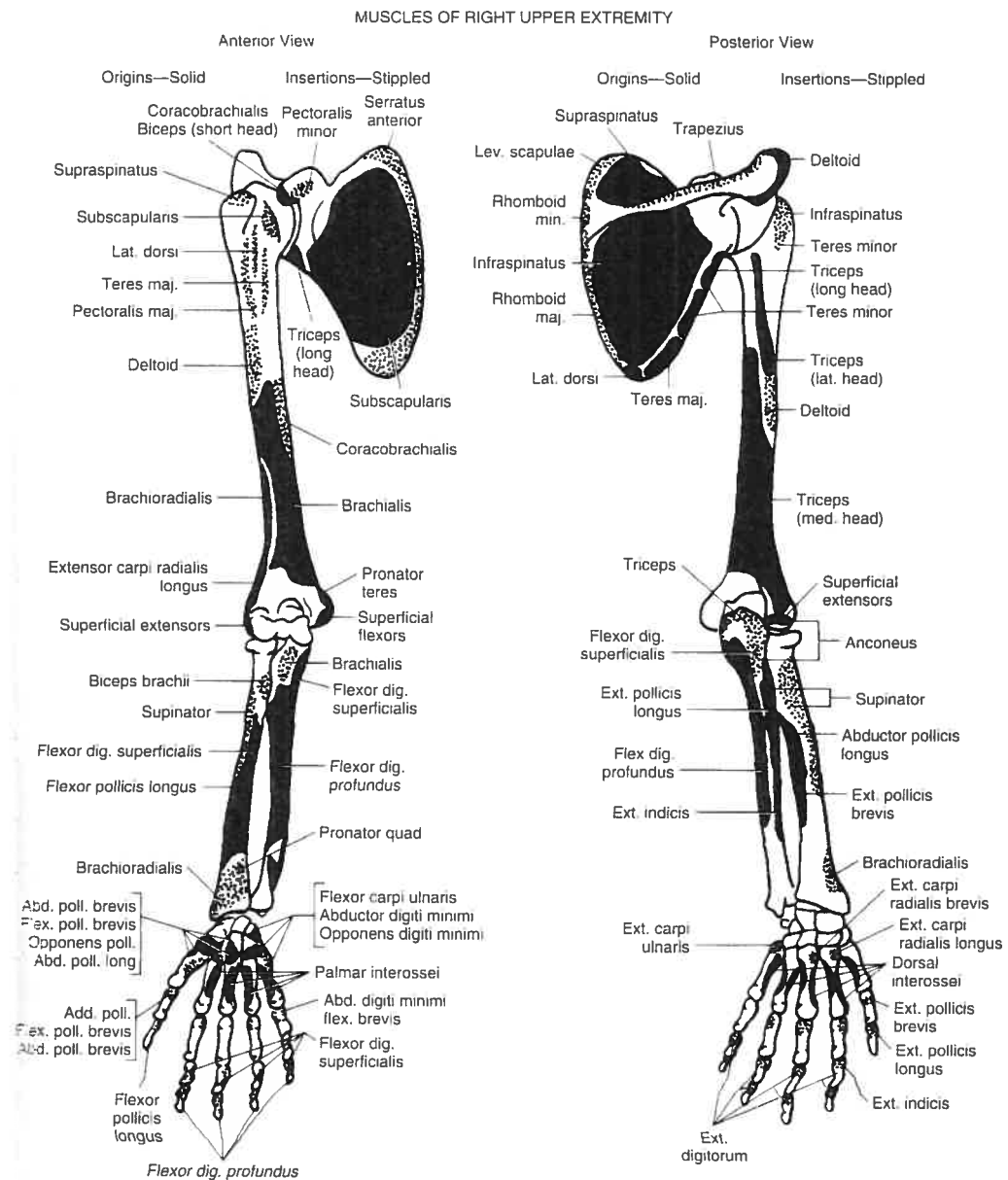
The mechanosensitivity of chondrocytes allows local bone growth rates to adapt bone and joint form to the mechanical environment. The process is site specific, responding to the characteristics of recent habitual local loads. Chondral modelling affects the longitudinal growth of bones from cartilage at the growth plate, as well as articular surface growth. Joint shape and size can be altered while joint congruence is maintained to prevent damage of articular and underlying bone. Through chondral modelling the hydrostatic compressive stresses exerted on chondrocytes during cartilage compression influence joint conformation. Mechanotransduction regulates the rate of chondrocyte maturation and metabolism, affecting local rates of bone growth adjacent to cartilage at the growth plate and articular surfaces (Plochocki, 2003).

1.4 Muscle attachments

Muscle attachment sites are often distinct skeletal markings and bony projections that occur where a muscle, a tendon, or a ligament inserts into the blood-supplying periosteum and underlying bony cortex (Hawkey and Merbs, 1995; Hawkey, 1998; Wilczak, 1998a, b; Knusel, 2000; Eshed et al., 2003; Weiss 2003, 2004; Zumwalt, 2005; Molnar, 2006;). These attachment sites, also called entheses, are the main visible records of muscles on the skeleton and may be an important record of human behaviour (Figure III).

It has been assumed in biological anthropology that the expression of muscle attachment sites is indicative of the relative size, strength, or activity of the attaching muscles (Hawkey and Merbs, 1995; Hawkey, 1998). When muscle insertion sites are subjected to stress, blood flow is increased, which stimulates bone forming cells that results in bone hypertrophy and increased size of musculoskeletal markers (Hawkey, 1998; Wilczak, 1998a, b). These markers can be used by anthropologists and paleontologists to interpret evolutionary history, prehistory, locomotor and manipulative adaptations of humans and other species as well as occupational pathologies, since muscle attachments are the result of continued muscle use in daily and repetitive tasks, which makes them ideal for reconstructing past lifestyles.

Figure III: Muscle attachment sites of the upper limbs (from Nordin and Frankel, 2001).



Muscle attachment sites can be studied in inter-specific comparisons of the relative sizes and positions of muscle or tendon attachment sites used to reconstruct functional morphology and evolutionary change. Muscle markers variation can also be studied within a single population to reconstruct the activity patterns of the individuals in the groups. In order to be able to use

muscle attachments as a proxy of mechanical loadings, which in turn are hypothesized to affect the articular surfaces, muscle markers must be well understood (Zumwalt, 2005). Therefore, the following describes the effect of muscle contraction on the bone.

The stress on a surface equals the amount of force applied to that surface, divided by the area across which the force is applied. It is advantageous for bony attachment sites to increase in size to reduce stresses incurred by high muscle forces (Zumwalt, 2005). For example, on the surface of some primate skulls, sagittal bony crests build up during growth. These crests serve to enlarge the surface area for insertion of the *temporalis* (chewing) muscles and develops only if the muscle is enlarged enough to meet on top of the skull (Ankel-Simons, 2000). Some experimental studies support the idea that muscle force directly affects attachment site morphology. For example, the effect of muscle size on attachment morphology was examined in mice in which myostatin, a negative-regulator of skeletal muscle growth, had been genetically knocked out (Hamrick et al, 2000). The myostatin-null mice exhibited a doubling of muscle mass as well as larger femoral third trochanters as compared to normal mice. Bone will respond to stimuli differently in different conditions, but the overall evidence of bone plasticity is consistent with mechanically induced musculoskeletal stress markers (MSM) hypertrophy. In addition muscle markers are the result of an accumulation of stresses experienced by an individual. As a result, activity can be correlated to the hypertrophy at muscle insertions (Wilczak, 1998b). Since muscle markers develop in response to muscle use and size, they can be used as a surrogate of the strength of the muscles.

1.5 Hypotheses to be tested

Loads in joints are incurred via muscle contraction and gravity. Body mass, because of gravity, contributes significantly to the mechanical demand on the articulations of the lower limbs. Since humans are bipedal, gravitational force has much less influence on the upper limbs. Thus, articulations of the upper limbs incur loads almost exclusively through muscle contractions. Humans are

usually either left handed or right handed and the use of a preferred side originates early in childhood. As a consequence, it is possible to identify the preferred side of an individual found in an archaeological context by comparing the size and development of right and left muscle insertions. Also, since muscle markers develop in response to muscle use and size, they can be used as proxy of the strength of the muscles.

Using muscle markers as surrogate for muscular strength, it is possible to determine whether articulations show a similar asymmetry. Previously, it was stated that, by responding to hydrostatic stresses, joint growth is hypothesized to follow a trajectory that reduces large loads per unit area while maintaining joint congruence through adaptations in joint size, shape, smoothness and curvature (Frost, 1999; Hamrick, 1999b). Since very few studies have been able to demonstrate directly the influence of mechanical strain on the shape of joints in humans, this study further investigates the plasticity of articular surfaces. This project tests whether size and/or the shape of the articulations of the upper limbs change according to the forces that cross them. As stated above, muscle markers are used as proxy to muscle contraction strength and frequency.

The null hypothesis is:

H_0 = There is no right-left differences in articular surfaces of the upper limbs in humans relative to the difference in loads incurred by each side.

Two alternative hypotheses derive from the null hypothesis. They are not mutually exclusive and can both be supported.

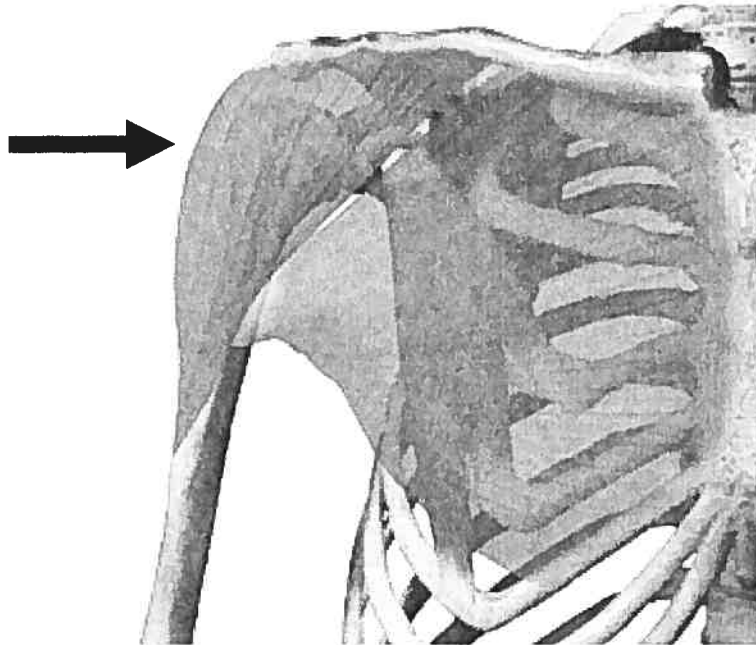
H_1 = The right-left *shape* differences in articular surfaces of the upper limbs in humans vary relative to the difference in loads incurred by each side.

H_2 = The right-left *size* differences in articular surfaces of the upper limbs in humans vary relative to the difference in loads incurred by each side.

Individuals with larger muscle markings should develop flatter and larger articular surfaces to better distribute the larger loads induced by muscle contractions. For example, muscles surrounding the shoulder (ex. the *deltoideus*, the rotator cuff muscles) push medially the humeral head when they

contract. These contractions cause the humeral head to compress the glenoid surface of the scapula (Figure IV). As a consequence of these forces, the glenoid surface and the humeral head should have a larger articular surface and the glenoid cavity should also be flatter.

Figure IV: Example of muscle contraction shown by the *deltoideus* (above-left) and the *pectoralis major* (below-right) on the shoulder joint causing the head of the humerus to compress the glenoid surface of the scapula. The black arrow represents the medially directed load from the muscular contraction acting on the shoulder articulation. Figure shows anterior view of the shoulder (from Sénécal, 2003).



However, the situation would be different at the elbow (Figure V). For example, many wrist and finger flexor muscles cross the joint diagonally (dashed arrows). The transverse force vectors (full arrow) of these muscles act to dislocate the ulna from the humerus. In order to stabilize the articulation, the medial keel of the trochlea on the humerus is extended (Figure VI) to prevent the ulna from being displaced medially. For this articulation, greater muscle contractions should result in an acute angle of the inferior surface of the humeral trochlea with a longer medial as well as a lateral trochlear lip. As

predicted for the shoulder, the distal articular surface of the humerus is hypothesized to increase in size in order to better resist the loads.

Figure V: Example of the muscle contractions caused by the flexors and extensors of the forearm acting on the elbow articulation (from Platzer, 2001). Figures show anterior views of the elbow.

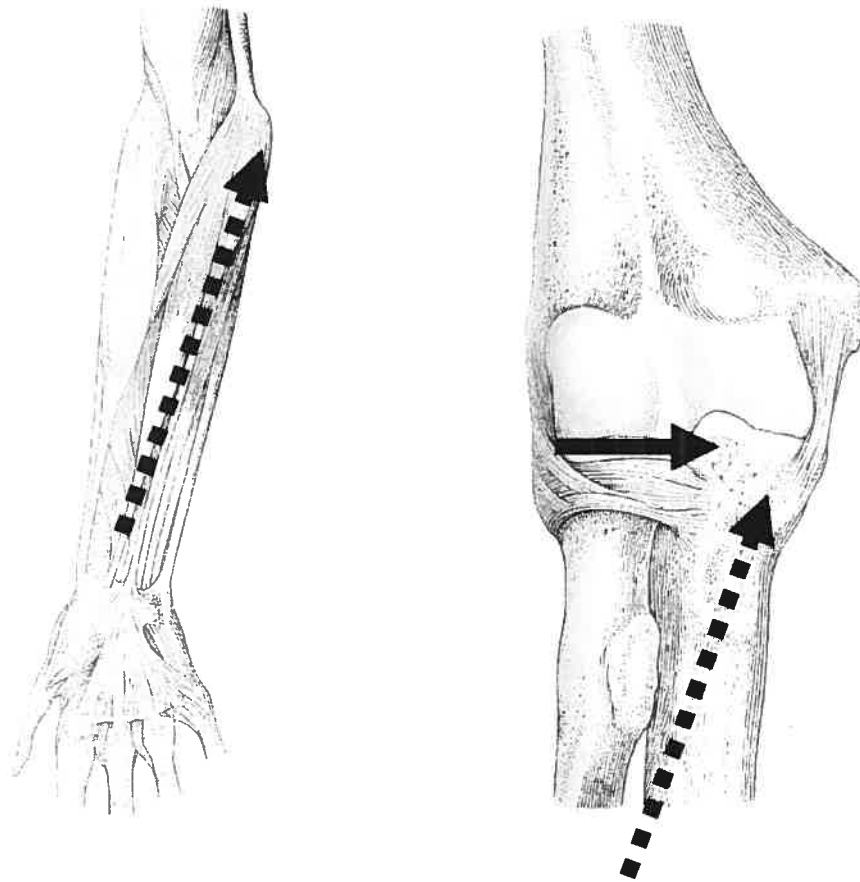
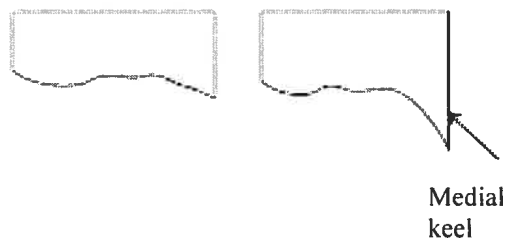
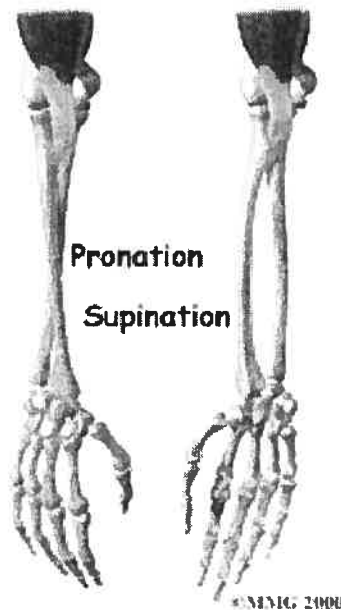


Figure VI: Schematic illustration showing a strong medial keel on the elbow articulation (from Schmitt, 2003).



At the humero-radial articulation, the head of the radius rotates around the humeral surface as it accompanies the ulna during flexion-extension movement, and spins on the humeral surface during pronation and supination. During pronation-supination (Figure VII) the radial head spins in place, while the distal radius rotates around the distal ulnar head at the distal radio-ulnar articulation. Supination (rotation of the hand medially) takes place at the humero-radial and proximal radio-ulnar joints with the radius rotating about a longitudinal axis passing through the centre of the capitulum and the radial head and the distal ulnar head (Nordin and Frankel, 2001). It is expected that the surface of the radial head should have a larger but flatter articular surface when there is more frequent muscle contraction. The proximal and distal radio-ulnar articulations should have the same response to the greater muscle loadings. They are predicted to develop larger and flatter articular surfaces with recurrent and powerful muscle contractions.

Figure VII: Pronation (rotation of the hand laterally) and supination (rotation of the hand medially) movements of the forearm (from DePuy Orthopaedics, 2005).



The radio-carpal and carpo-metacarpal articulations are expected to develop flatter and/or larger articular surfaces as well to better distribute the greater loads induced by contraction of the muscles crossing the wrist and the hand.

In general, at each joint, it is expected to see a generally larger articular surface on the preferred side and that may have a different form, which is usually predicted to be flatter except for the humero-ulnar articulation.

Chapter 2: Materials and methods

2.1 Materials

The skeletal collection (Table 1) used in this study is archaeological and of mixed ancestry. Both males and females were included. The sample integrated only non-pathological individuals. Juveniles were not included because during growth, tendons and ligaments attach primarily to the periosteum, which is attached to the bone by a relatively small number of collagen fibres. Only after epiphyseal growth plates close and growth is complete do the tendons and ligaments of long bones pass through the periosteum and attach firmly to the underlying bone. This mechanism allows the attachment of soft tissue to migrate relatively easily during growth to maintain a constant position to the growth plate and adjacent joints. As a result, the morphologies of juvenile muscle attachment sites are unlikely to reflect fully the size or activity of the attaching muscle (Zumwalt, 2005). The stress of activity patterns accumulates over time, so older individuals have more pronounced muscle markers than younger individuals. In order to avoid measuring individuals that have greater markings simply because of their age or individuals whose activity levels might have decreased during life due to advanced age; the individuals approximately over 50 years were not included. The sample was aged and sexed using museum records. All specimens are housed at the Canadian Museum of Civilization, except for three (all Euroamericans) that are housed at the Paleoanthropology Laboratory of the Université de Montréal.

Table 1: Study sample

Groups	Females	Males	Indeterminate	Sample size
Sadlermiut Inuit (Nunavut)	18	13	0	31
Amerinds (British-Columbia, Manitoba, Ontario)	13	29	5	47
Euroamericans	4	25	1	30
Total	35	67	6	108

2.2 Methods

The bones used in the analysis are: the clavicle, scapula, humerus, ulna, radius, as well as the first, second and third metacarpal. The articulations investigated are: gleno-humeral, humero-ulnar, humero-radial, proximal and distal radio-ulnar, and carpo-metacarpal of the three radial digits. An osteometric board was used to measure the bone length to the nearest 0.5mm and the articular surface measurements were taken with sliding calipers and recorded to the nearest 0.1mm (Table 2). Measures were taken using the methods described in Martin and Saller (1957).

Table 2: Linear measurements

Linear measurement	Abbreviation
SI* height of glenoid surface	SGSI
AP length of the glenoid surface	SGAP
SI height of humeral head	HHSI
AP length of humeral head	HHAP
ML width distal articular surface	HDML
ML width of the trochlea	HTML
SI height of the capitulum	HCSI
SI height of the zona conoidea	HZSI
SI height of the trochlear surface	HTSI
ML width superior portion of proximal ulna articular surface	UTML
ML width inferior portion of proximal ulna articular surface	URML
ML width at mid-portion of proximal ulna articular surface	ULAT
SI height of trochlear notch	UTSI
SI height of radial notch on the ulna	RNSI
AP length of radial notch on the ulna	RNAP
ML width of ulnar distal articular surface	UNML
AP length of ulnar distal articular surface	UNAP
ML width of radial head	RHML
AP length of radial head	RHAP
ML width of radiocarpal surface	RDML
AP length of radiocarpal surface medial side	RDAP
AP length of mid radiocarpal surface	RDAPM
ML width of first metacarpal head	MC1HML
AP length of first metacarpal head	MC1HAP
ML width of first metacarpal base	MC1BML
AP length of first metacarpal base	MC1BAP
ML width of second metacarpal head	MC2HML
AP length of second metacarpal head	MC2HAP
ML width of second metacarpal base	MC2BML
AP length of second metacarpal base	MC2BAP
ML width of first proximal phalange base	PBML
AP length of first proximal phalange base	PBAP

*SI: supero-inferior. AP: antero-posterior. ML: medio-lateral

When comparing the articular size, only one variable per articulation was included. When possible an average value for the two measures (ex. SI

height and AP length of the glenoid surface) for one joint was used as the size variable. The combination of the two measures could only be done if they were thought to reflect accurately the overall size of the articulation. As for the articular shape analysis all angles measured on one articulation were analyzed separately in order to better understand how the surfaces may be modified to better resist loads.

Joint shape was recorded using a digitizer (Microscribe G2X). Data was collected on the glenoid surface (Figure VIII), on the distal humerus (Figure IX), on the proximal and distal radius (Figure X and XI), and on the proximal first (Figure XII) and third metacarpals. On the third metacarpal, the points were the same as on the first, except that the posterior point was taken on the styloid process. Angles were calculated from these three-dimensional points and were analyzed to determine whether the shape of an articular surface might be different due to the different mechanical environment. Angle C of the distal humerus was calculated using digital pictures (Figure IX).

Muscle marker size is used as a surrogate for the changes incurred by the articulations during life. The attachments included the area covered by the tendinous attachment and the areas immediately adjacent to this attachment that show formation of new bone on the smooth cortical surface (Table 3). Wilczak's method (1998a, b) was used to measure most of the maximum length and width of the attachments. The maximum length was aligned vertically by placing the sliding callipers at the most superior and inferior points of each insertion. The maximum width was aligned by placing the sliding clippers on either side of the widest point perpendicular to the maximum length (Wilczak, 1998b). In addition, the maximum projection of the coracoid process and the acromion as well as the projection of the medial and lateral epicondyles were taken. The maximum projection was aligned by placing the sliding callipers on the associated articulation to the end of the bony projection. There are limitations to using quantitative estimates of insertion size (Wilczak, 1998a, b; Zumwalt, 2005). Since bone is a three-dimensional structure, information about the morphology of the insertion site is lost and rugosity is not considered.

Figure VIII: Points taken on the shoulder, lateral view. The superior (1), middle (5) and inferior (3) points form the SI angle and the anterior (2), middle (5) and posterior (4) points form the AP angle.

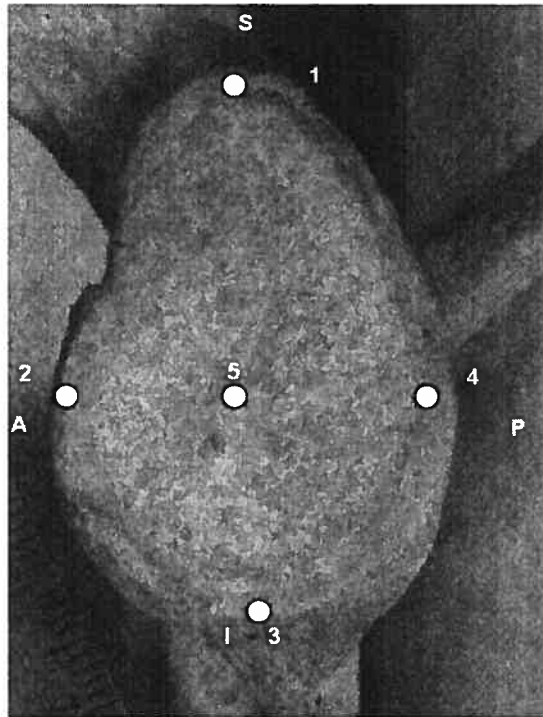


Figure IX: Points taken and angles calculated at the humero-ulnar articulation, anterior view. A - Inferior medial angle (points 1, 3, 2), B - Inferior lateral angle (points 1, 3, 4), and C - Medial angle of the humeral trochlea (points 2, 3, 4).

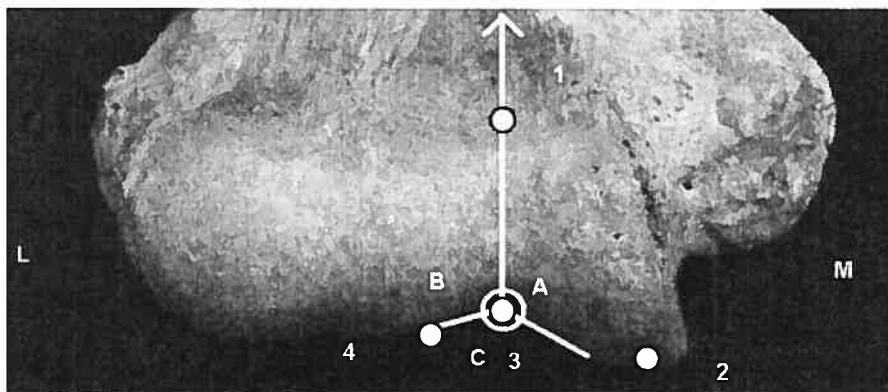


Figure X: Points taken at proximal surface of the radius, superior view. The medial (2), middle (5) and lateral (4) points form the ML angle and the anterior (1), middle (5) and posterior (3) points form the AP angle.

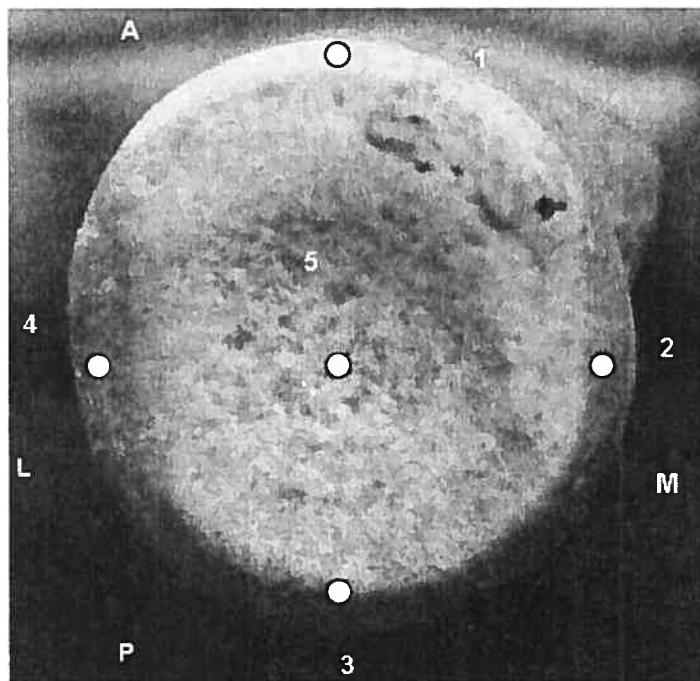


Figure XI: Points taken at the distal surface of the radius, inferior view. Anteriorly the medial (3), middle (6) and lateral (1) points form the ML angle 1 and ML angle 2 is posteriorly (1, 6, 4). The anterior (2), middle (6) and posterior (5) points form the AP angle.

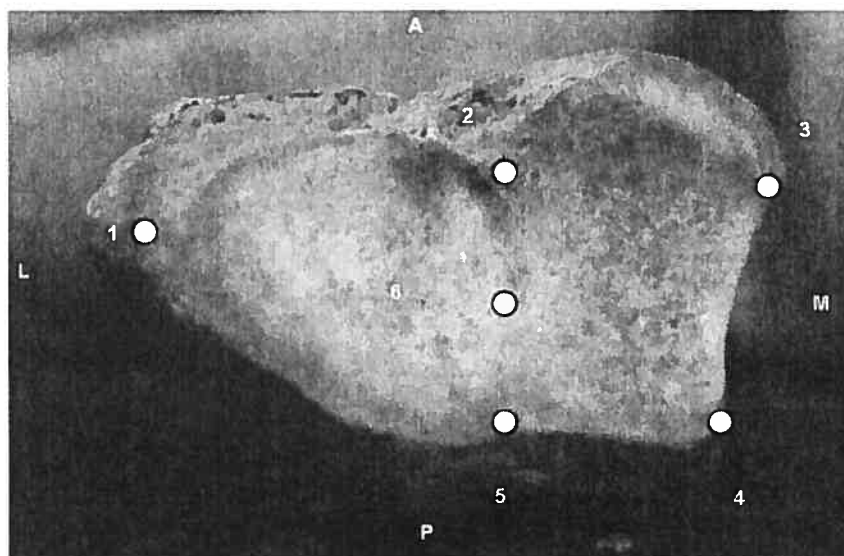


Figure XII: Points taken at the proximal surface of the first metacarpal, superior view. The medial (2), middle (5) and lateral (4) points form the ML angle and the anterior (1), middle (5) and posterior (3) points form the AP angle.

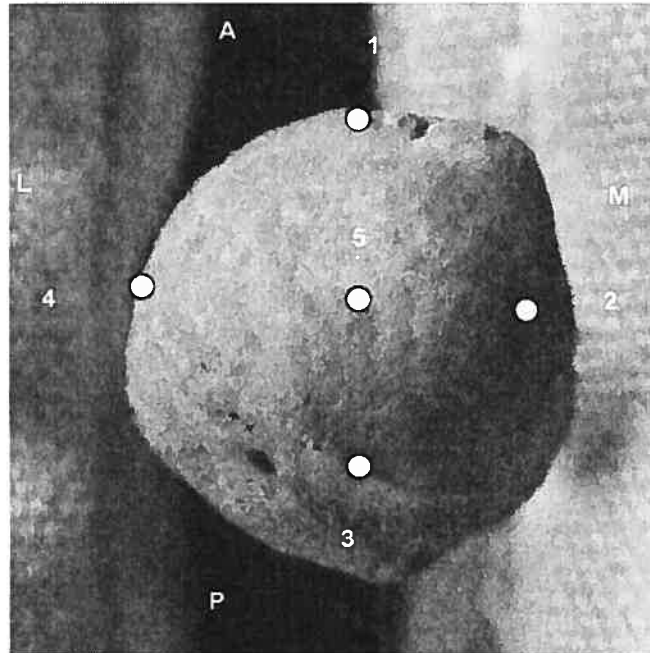


Table 3: Muscle attachments

Muscle	Corresponding structure measured
<i>Coracobrachialis, biceps brachii and pectoralis minor</i>	Coracoid process
<i>Deltoid and trapezius</i>	Acromion
<i>Subscapularis</i>	Lesser tubercle
<i>Teres minor, supraspinatus and infraspinus</i>	Greater tubercle
<i>Pectoralis major</i>	Insertion of the <i>pectoralis major</i>
<i>Deltoideus</i>	Insertion of the <i>deltoideus</i>
<i>Pronator teres, flexor carpi radialis, flexor carpi ulnaris, palmaris longus and flexor digitorum superficialis.</i>	Medial epicondyle
<i>Anconeus, brachioradialis, supinator, extensor carpi radialis longus, extensor carpi radialis brevis, extensor carpi ulnaris, extensor digitorum and extensor digiti minimi.</i>	Lateral epicondyle
<i>Biceps brachii</i>	Radial tuberosity
<i>Triceps brachii</i>	Olecranon
<i>Brachialis</i>	Ulnar tuberosity
<i>Pronator quadratus</i>	Insertion of the <i>pronator quadratus</i>
<i>Pronator teres</i>	Insertion of the <i>pronator teres</i>
<i>Supinator</i>	Insertion of the <i>supinator</i>
<i>Abductor pollicis longus</i>	Origin of the <i>abductor pollicis longus</i>

Three individuals were measured three times over a period of several weeks to test for measurement error (Table 4 and Table 5). Measurement errors were calculated using the method outlined by White and Folkens (2001) in which differences from the mean of the measurements are averaged and expressed as a percentage of the mean measure. All linear measurements for the articulations are under 3%. Muscle site measurements are all under 6% except for the lateral epicondyle projection, which ranges around 9%. This error is taken into consideration in the analysis.

Table 4: Measurement errors for the articular measurements of the left and right sides included in this study (n = 3 individuals).

Articulation measurements	Mean percentage of error		
	Right side	Left side	Average
SI* height of glenoid surface	0.21%	0.31%	0.26%
AP length of the glenoid surface	0.63	0.77	0.7
SI height of humeral head	0.54	0.20	0.37
AP length of humeral head	0.45	0.35	0.4
ML width distal articular surface	0.51	0.52	0.51
ML width of the trochlea	1.08	1.48	1.28
SI height of the capitulum	0.50	1.07	0.78
SI height of the zona conoidea	1.51	1.23	1.37
SI height of the trochlear surface	1.28	1.32	1.30
ML width superior portion of proximal ulna articular surface	0.61	0.98	0.79
ML width inferior portion of proximal ulna articular surface	0.79	0.67	0.73
ML width at mid-portion of proximal ulna articular surface	1.83	1.15	1.49
SI height of trochlear notch	1.92	1.76	1.84
SI height of radial articulation on the ulna	1.81	1.92	1.86
AP length of radial articulation on the ulna	2.12	1.94	2.03
ML width of ulnar distal articular surface	2.50	2.21	2.35
AP length of ulnar distal articular surface	2.87	2.37	2.62
ML width of radial head	1.45	2.15	1.8
AP length of radial head	1.41	2.34	1.87
ML width of radiocarpal surface	1.56	1.65	1.60
AP length of radiocarpal surface medial side	1.14	0.60	0.87
AP length of mid radiocarpal surface	0.92	0.24	0.58
ML width of first metacarpal head	1.24	1.14	1.19
AP length of first metacarpal head	1.16	1.08	1.12
ML width of first metacarpal base	1.50	1.79	1.64
AP length of first metacarpal base	1.92	1.68	1.8
ML width of second metacarpal head	1.62	1.46	1.54
AP length of second metacarpal head	1.73	1.24	1.48
ML width of second metacarpal base	0.73	0.99	0.86
AP length of second metacarpal base	0.67	1.27	0.97

*SI: supero-inferior, AP: antero-posterior, ML: medio-lateral

Table 5: Measurement errors for the muscle site measurements of the right and left sides included in this study (n = 3 individuals).

Muscle site measurements	Mean percentage of error		
	Right side	Left side	Average
Coracoid process	2.01%	1.15%	1.58%
Acromion	1.64	1.52	1.58
Lesser tubercle	3.42	3.70	3.56
Greater tubercle	0.77	1.47	1.12
Insertion of the <i>pectoralis major</i>	4.92	3.22	4.07
Insertion of the <i>deltoideus</i>	5.31	3.85	4.58
Medial epicondyle	6.34	4.19	5.26
Lateral epicondyle	9.46	9.23	9.34
Radial tuberosity	2.55	2.47	2.51
Olecranon	3.36	3.47	3.41
Ulnar tuberosity	1.51	2.99	2.25
Insertion of the <i>pronator teres</i>	1.29	1.31	1.30
Insertion of the <i>supinator</i>	5.46	5.19	5.32
Origin of the <i>abductor pollicis longus</i>	1.59	1.56	1.57

2.3 Analysis

Skeletal bilateral directional asymmetries (DA) are commonly used as indicators of the influence of the mechanical environment on bone. DA occurs when one side of the skeleton is consistently more developed than the other and is largely attributable to differential mechanical loading during growth. Humans are unique among primates in the magnitude of directional bilateral asymmetry exhibited on the upper limb, favouring one side (usually the right) over the other. Difference in asymmetry of muscular and articular surfaces was calculated using the following formula in order to control for the effect of size:

$$DA = (\text{right} - \text{left}) / (\text{right} + \text{left}) * 2000$$

Although there is no standard method of calculating DA, this method and similar variants, are commonly employed (Steele and Mays, 1995; Mays et al., 1999; Plochocki, 2002, 2004). Negative scores indicate left dominance, while positive score indicate right dominance of the individuals.

There is much debate concerning the relationship of muscle attachment with age, sex and geographic origins (Hawkey and Merbs, 1995; Wilczak, 1998a, b; Eshed et al., 2003; Ruff, 2003; Weiss, 2003, 2004; Zumwalt, 2005; Molnar, 2006). DA was used in this project to concentrate muscular contractions by controlling for those factors that may influence the size of the muscle markers. Also, as seen in chapter 1, muscle attachment sites can be studied in inter-specific comparisons of the relative sizes and positions of

muscle or tendon attachment sites used to reconstruct functional morphology and evolutionary change (Zumwalt, 2005). Therefore, in order to study the functional morphology of the upper limb joints, all of the variation in the sample was combined.

For each articulation, only the muscles crossing at that particular articulation were used as the surrogate of muscular force. The measurements for the coracoid process, acromion, lesser and greater tubercle, and insertions of the *pectoralis major* and the *deltoideus* were correlated with the shoulder articulation measurements. The medial and lateral epicondyle, along with the radial and ulnar tuberosities, the olecranon, and the insertions of the *supinator* and the *pronator teres* were correlated with the elbow articulation measurements. The medial and lateral epicondyles and the origin of the *abductor pollicis longus* measurements were correlated with the wrists joint measurements. Finally, the lateral and medial epicondyles were correlated with the second or third metacarpal and the origin of the *abductor pollicis longus* was correlated with the first metacarpal.

Least-square regression is used to evaluate the influence of muscle size on joint shape and size. Statistical significance was set at 0.05 in all tests. All analysis were done using SPSS for Windows statistical software version 13.0. The number of individuals in each analysis varied due to the fact that the sample used is archaeological and fragmentary.

Chapter 3: Results

3.1 Shoulder: size

As shown in Table 6, only one significant relationship was found at the shoulder. The humeral head correlates positively ($p = 0.028$, $r = 0.279$) with the asymmetry of the greater tubercle (Figure XIII). This positive correlation indicating a greater size of the humeral head with larger muscle attachment is as hypothesized.

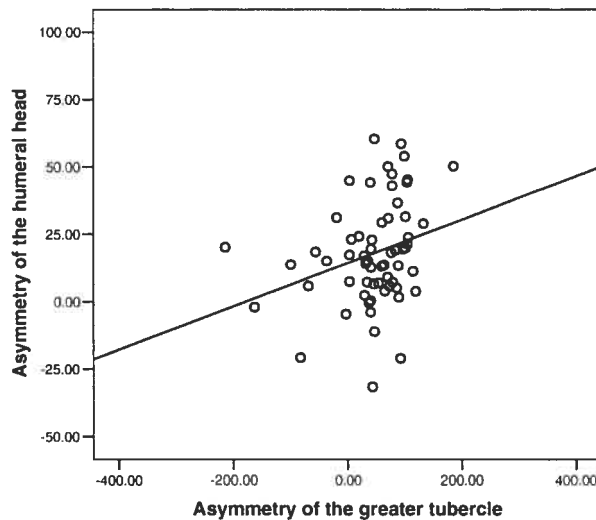
The size of the glenoid surface is close to have a significant negative relationship with the size of the coracoid process ($p = 0.08$, $r = 0.314$). This negative correlation indicating a smaller surface area of the glenoid cavity with increasing muscle marking size is contrary to what is expected.

Table 6: Correlation coefficients and significance of the regressions of articular size and muscle attachment size at the shoulder

Muscle/Independent variable	Glenoid surface				Humeral head			
	n*	P	b	r	n	p	b	r
Coracoid process	32	0.080	-0.173	0.314	32	0.310	-0.046	0.185
Acromion	39	0.532	0.039	0.103	40	0.530	-0.025	0.102
Lesser tubercle	56	0.837	0.010	0.028	68	0.309	-0.027	0.125
Greater tubercle	49	0.826	-0.018	0.032	62	0.028	0.080	0.279
Insertion of <i>pectoralis major</i>	59	0.708	0.010	0.050	72	0.875	-0.002	0.019
Insertion of <i>deltoideus</i>	66	0.517	0.018	0.081	73	0.364	0.014	0.108

*n: number of individuals with paired skeletal elements, p: statistical significance, b: regression coefficient (slope value), r: correlation coefficient

Figure XIII: Regression between size of the humeral head and the size of the greater tubercle.



3.2 Elbow; size

There are a few more significant relations at the elbow (Tables 7, 8 and 9). At the distal humerus, the height of the capitulum ($p = 0.030$, $r = 0.243$) correlates positively with the size of the lateral epicondyle (Figure XIV). This positive correlation indicating a larger surface area of the capitulum with increasing muscle attachment size is as expected. However, the height of the capitulum ($p = 0.033$, $r = 0.285$) and the size of the trochlea, which is the combination of the SI and ML measurements of the trochlea ($p = 0.002$, $r = 0.363$), correlates negatively with the insertion for the *pronator teres* (Figures XV) and the olecranon (Figure XVI) respectively. As it can be seen, the size of the trochlea and the olecranon size have a pretty strong negative relationship. The ML width of the distal articular surface of the humerus is close to have a significant negative relationship with the size of the medial epicondyle ($p = 0.068$, $r = 0.197$). These negative relationships are contrary to what was expected. At the distal elbow, many measurements show that the articular surfaces are reduced in size with greater muscular contractions.

Table 7: Correlation coefficients and significance of the regressions of articular size and muscle attachment size at the distal humerus

Muscle/ Independent variable	ML width distal articular surface				SI height of the capitulum			
	n*	p	b	R	n	p	b	r
Medial epicondyle	87	0.068	-0.020	0.197	83	0.755	0.007	0.035
Lateral epicondyle	82	0.287	-0.010	0.119	80	0.030	0.041	0.243
Radial tuberosity	75	0.880	0.003	0.018	73	0.141	-0.054	0.174
Olecranon	72	0.659	0.008	0.53	73	0.745	-0.013	0.039
Ulnar tuberosity	78	0.704	0.007	0.044	76	0.105	-0.057	0.188
Insertion of <i>pronator teres</i>	59	0.352	-0.009	0.123	56	0.033	-0.044	0.285

Muscle/ Independent variable	SI height of the zona conoidea				Trochlea			
	n	p	B	r	n	p	b	r
Medial epicondyle	85	0.787	-0.005	0.030	82	0.515	-0.017	0.072
Lateral epicondyle	80	0.203	-0.022	0.148	76	0.809	-0.005	0.027
Radial tuberosity	75	0.385	0.029	0.105	70	0.349	-0.038	0.110
Olecranon	75	0.002	-0.104	0.363	72	0.824	-0.009	0.026
Ulnar tuberosity	78	0.374	-0.028	0.104	75	0.624	0.018	0.056
Insertion of <i>pronator teres</i>	58	0.183	-0.025	0.184	54	0.858	-0.004	0.224

*n: number of individuals with paired skeletal elements. p: statistical significance. b: regression coefficient (slope value). r: correlation coefficient

Figure XIV : Regression between the size of the SI height of the capitulum and the size of the lateral epicondyle.

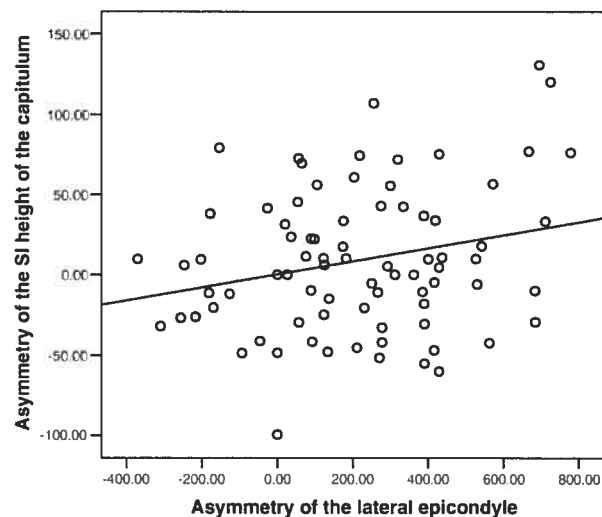


Figure XV: Regression of the size of the SI height of the capitulum and the size of the insertion of the *pronator teres* muscle.

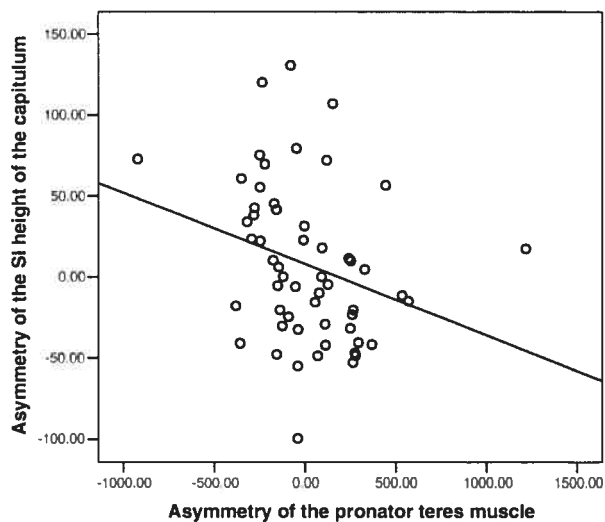
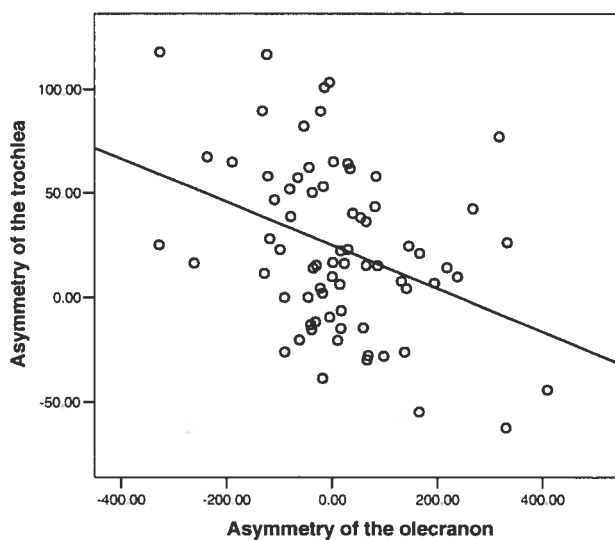


Figure XVI: Regression between the size of the trochlea and the size of the olecranon.



There are no significant relationships at the proximal ulnar measurements (Table 8). Only the ML width of the inferior portion of the proximal ulna articular surface is close to having a significant positive relationship with the olecranon ($p = 0.088$, $r = 0.210$). This correlation agrees with the expectations since a greater width was hypothesized with greater muscle markings.

Table 8: Correlation coefficients and significance of the regressions of articular size and muscle attachment size at the proximal ulnar measurements

Muscle/ Independent variable	Trochlear notch				ML width inferior portion of proximal ulna articular surface			
	n*	p	b	r	N	p	b	r
Medial epicondyle	73	0.319	0.033	0.118	70	0.607	-0.026	0.063
Lateral epicondyle	66	0.709	0.009	0.047	65	0.786	0.010	0.034
Olecranon	67	0.329	- 0.051	0.121	67	0.088	0.139	0.210
Ulnar tuberosity	72	0.697	0.017	0.047	72	0.754	-0.020	0.038
Radial tuberosity	69	0.180	- 0.059	0.163	71	0.644	-0.033	0.056
Insertion of <i>pronator teres</i>	52	0.544	- 0.019	0.086	56	0.717	-0.016	0.050

Muscle/ Independent variable	ML width at mid-portion of proximal ulna articular surface			
	n	P	b	r
Medial epicondyle	77	0.690	-0.012	0.046
Lateral epicondyle	70	0.651	0.010	0.055
Olecranon	75	0.645	0.021	0.054
Ulnar tuberosity	79	0.217	-0.048	0.141
Radial tuberosity	77	0.627	-0.020	0.056
Insertion of <i>pronator teres</i>	60	0.188	-0.033	0.172

*n: number of individuals with paired skeletal elements. p: statistical significance. b: regression coefficient (slope value). r: correlation coefficient

As shown in Table 9, two significant relations are observed at the articulations of the proximal ulna and radius. The size of the radial head correlates positively ($p = 0.045$, $r = 0.265$) with the size of the radial tuberosity (Figure XVII). A greater surface area of the radial head with a greater muscle attachment was predicted. As for the size of the radial notch found on the ulna, it correlates negatively ($p = 0.043$, $r = 0.233$) with the insertion of the *supinator*

(Figure XVIII). The size of the radial head comes close to a significant negative correlation ($p = 0.089$, $r = 0.234$) with the size of the medial epicondyle. These results indicating a smaller surface area of the radial notch and the radial head with increasing muscle marking size is contrary to what was expected.

Table 9: Correlation coefficients and significance of the regressions of articular size and muscle attachment size at the proximal ulna and radius

Muscle/ Independent variable	Radial notch				Radial head			
	n*	p	B	r	n	p	b	r
Medial epicondyle	74	0.160	0.082	0.165	54	0.089	-0.053	0.234
Lateral epicondyle	69	0.412	-0.036	0.100	50	0.125	-0.038	0.220
Olecranon	74	0.328	0.076	0.115	52	0.700	0.019	0.055
Ulnar tuberosity	77	0.762	-0.023	0.035	58	0.120	0.061	0.206
Radial tuberosity	73	0.931	-0.007	0.010	58	0.045	0.079	0.265
Insertion of <i>pronator teres</i>	57	0.179	-0.070	0.181	53	0.697	0.007	0.055
Insertion of <i>supinator</i>	76	0.043	-0.079	0.233	58	0.150	0.029	0.192

*n: number of individuals with paired skeletal elements. p: statistical significance, b: regression coefficient (slope value). r: correlation coefficient

Figure XVII: Regression between the size of the radial head and the size of the radial tuberosity.

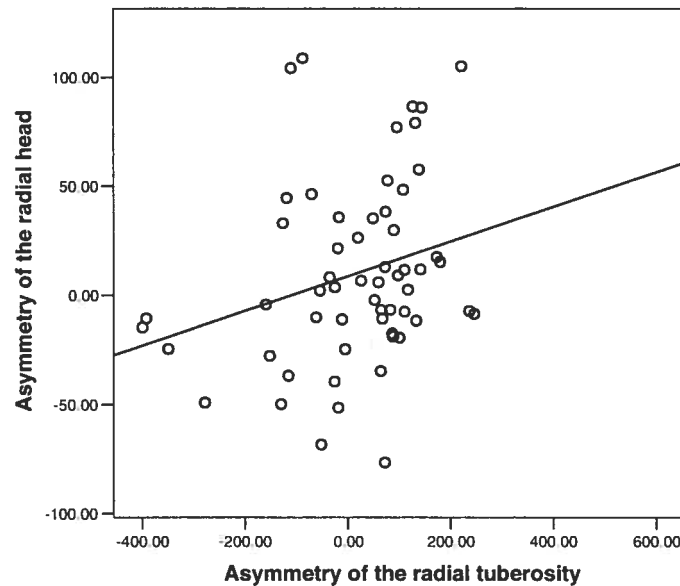
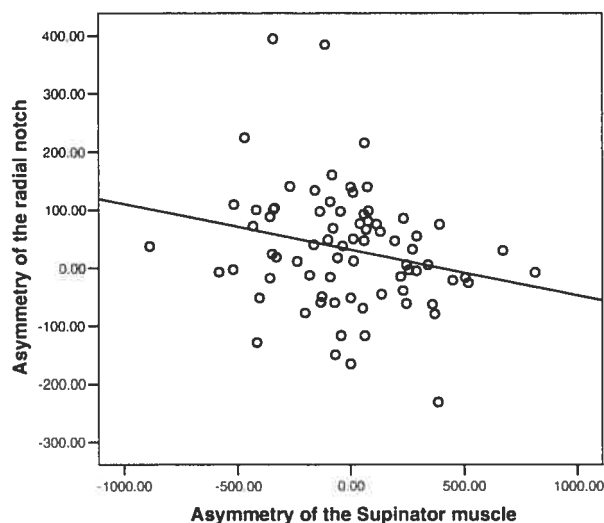


Figure XVIII: Regression between the size of the radial notch and the size of the insertion of the *supinator* muscle.



3.3 Wrist; size

There is no significant relationship at any of the wrist articulations (Table 10). There is no relation that is close to being significant.

Table 10: Correlation coefficients and significance of the regressions of articular size and muscle attachment size at the wrist

Muscle/ Independent variable	ML width of radio-carpal surface				AP length of radio-carpal surface medial side			
	n*	p	b	r	n	p	b	R
Medial epicondyle	68	0.606	-0.034	0.064	69	0.299	-0.067	0.127
Lateral epicondyle	66	0.430	-0.039	0.099	67	0.954	0.002	0.007
Insertion of <i>abductor pollicis longud</i>	70	0.798	0.010	0.031	72	0.893	0.005	0.016

Muscle/ Independent variable	AP length of mid radio-carpal surface				Ulnar head			
	n	p	b	r	n	p	B	r
Medial epicondyle	61	0.475	-0.043	0.093	58	0.881	0.007	0.020
Lateral epicondyle	60	0.953	-0.003	0.008	53	0.915	0.004	0.015
Insertion of <i>abductor pollicis longud</i>	65	0.415	0.032	0.103	60	0.175	0.047	0.177

*n: number of individuals with paired skeletal elements. p: statistical significance. b: regression coefficient (slope value). r: correlation coefficient

3.4 Hand; size

There is no significant relationship either at any of the hand articulations (Table 11). There is no relation that is close to being significant.

Table 11: Correlation coefficients and significance of the regressions of articular size and muscle attachment size at the hand

Muscle/ Independent variable	Head of Mc1				Base of Mc1			
	n*	p	b	R	n	p	b	r
Insertion of <i>abductor pollicis longus</i>	53	0.768	0.007	0.041	49	0.161	-0.078	0.208

Muscle/ Independent variable	Head of Mc2				Base of Mc2			
	n	p	b	R	n	p	b	r
Medial epicondyle	47	0.757	-0.024	0.050	54	0.173	0.001	0.188
Lateral epicondyle	32	0.310	0.024	0.169	67	0.930	0.004	0.013

*n; number of individuals with paired skeletal elements, p; statistical significance, b; regression coefficient (slope value), r; correlation coefficient

Therefore, when looking at the size of the joint in relation to muscular insertion size, significant relationships were found only at the shoulder and elbow.

3.5 Shoulder; shape

Table 12 shows no significant relationship in the different angles of the glenoid cavity in relation to the muscular contractions at the shoulder. The SI angle of the glenoid surface has a positive relationship close to significant ($p = 0.084$, $r = 0.310$) with the coracoid process. This result in a less concave surface of the glenoid cavity as it was expected. It is however the only relationship close to being significant at this joint.

Table 12: Correlation coefficients and significance of the regressions of articular shape and muscle attachment size at the glenoid cavity

Muscle/Independent variable	Angle SI				Angle A-P			
	n	p	B	r	n	p	b	r
Coracoid process	33	0.084	0.031	0.310	35	0.593	0.122	0.095
Acromion	41	0.730	0.673	0.119	41	0.120	0.175	0.250
Lesser tubercle	59	0.460	0.030	0.100	58	0.165	0.032	0.187
Greater tubercle	52	0.443	-0.309	0.110	54	0.814	-0.057	0.033
Insertion of <i>pectoralis major</i>	62	0.716	-0.079	0.048	63	0.354	-0.077	0.121
Insertion of <i>deltoideus</i>	69	0.414	0.077	0.103	69	0.917	-0.268	0.013

*n: number of individuals with paired skeletal elements, p; statistical significance, b; regression coefficient (slope value), r; correlation coefficient

3.6 Elbow; shape

Table 13 shows that the inferior lateral angle of the humeral trochlea is positively correlated with both the ulnar tuberosity ($p = 0.017$, $r = 0.332$; Figure XIX) and the radial tuberosity ($p = 0.031$, $r = 0.312$; Figure XX). The inferior lateral angle of the humeral trochlea is also close to having a positive significant relationship with the olecranon ($p = 0.081$, $r = 0.257$). This indicates that the lateral lip of the distal humerus becomes more vertical to resist the greater muscular contractions as was predicted. The inferior medial angle of the humeral trochlea is also close to a significant negative correlation ($p = 0.086$, $r = 0.091$) with the size of the lateral epicondyle. This indicates that contrary to what was expected, the medial lip of the distal humerus becomes more horizontal to resist the greater muscular contractions. However, the correlation coefficient is very low ($r = 0.091$), indicating that muscle contractions by the elbow extensors do not greatly influence the angle of the medial lip.

Table 13: Correlation coefficients and significance of the regressions of articular shape and muscle attachment size at the distal humerus

Muscle/ Independent variable	Inferior medial angle of the humeral trochlea (A)				Inferior lateral angle of the humeral trochlea (B)				Medial angle of the humeral trochlea (C)			
	n	p	b	r	n	P	b	r	n	p	b	r
Medial epicondyle	49	0.220	- 0.018	0.024	49	0.836	- 0.009	0.030	51	0.792	0.006	0.038
Lateral epicondyle	48	0.086	- 0.043	0.091	46	0.227	- 0.050	0.181	51	0.523	0.016	0.043
Olecranon	47	0.103	0.069	0.108	47	0.081	0.123	0.257	49	0.358	- 0.039	0.136
Ulnar tuberosity	50	0.523	0.022	0.013	51	0.017	0.137	0.332	53	0.926	0.004	0.057
Radial tuberosity	48	0.222	0.048	0.049	48	0.031	0.134	0.312	50	0.571	0.019	0.056
Insertion of <i>pronator teres</i>	38	0.868	0.003	0.096	39	0.832	- 0.006	0.035	41	0.552	- 0.014	0.083

*n: number of individuals with paired skeletal elements, p: statistical significance, b: regression coefficient (slope value), r: correlation coefficient

Figure XIX: Regression of the shape values of the inferior lateral angle (B) of the humeral trochlea and ulnar tuberosity.

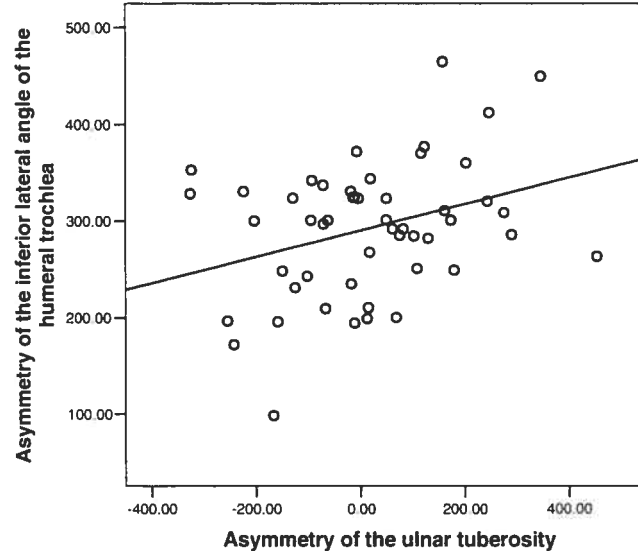


Figure XX: Regression of the shape values of the inferior lateral angle of the humeral trochlea (B) and the radial tuberosity.

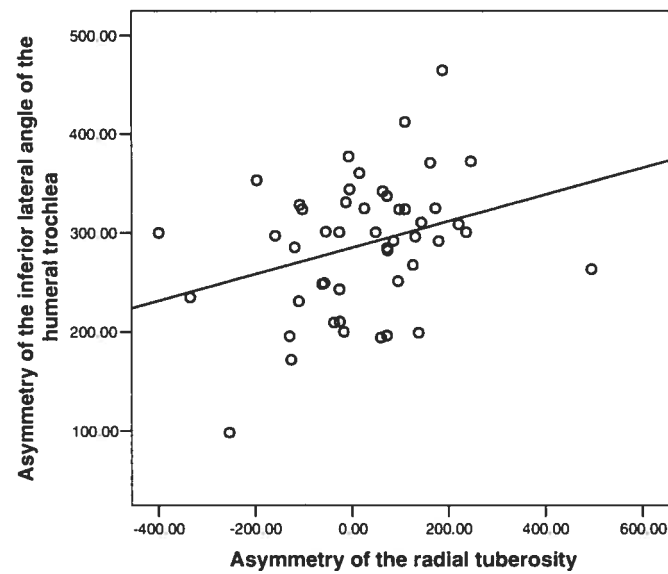


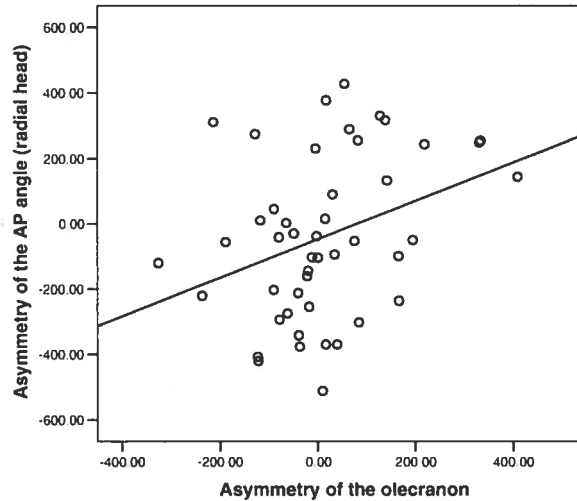
Table 14 shows a strong positive correlation between the AP angle of the radial head ($p = 0.019$, $r = 0.342$) and the olecranon (Figure XXI). The ML angle of the radial head has an almost significant positively correlated relationship ($p = 0.055$, $r = 0.285$) with the lateral epicondyle. The AP angle has a close to significant positive correlation ($p = 0.097$, $r = 0.311$) with the size of the ulnar tuberosity. These results indicate a larger AP or ML angle with stronger muscle contraction as expected. However, the ML angle of the radial head almost has a significant negatively correlated relationships with the ulnar tuberosity ($p = 0.088$, $r = 0.234$) and the insertion of the *pronator teres* ($p = 0.078$, $r = 0.282$). These go against the two previous results and the predictions, and the outcome is an acute angle, or more concave surface, correlated with stronger muscular contractions.

Table 14: Correlation coefficients and significance of the regressions of articular shape and muscle attachment size at the radial head

Muscle/ Independent variable	Radial head (AP angle)				Radial head (ML angle)			
	n*	P	B	R	n	p	b	r
Medial epicondyle	52	0.211	-0.324	0.176	49	0.111	0.055	0.228
Lateral epicondyle	45	0.149	-0.222	0.218	46	0.055	0.062	0.285
Olecranon	47	0.019	0.589	0.342	48	0.221	-0.065	0.178
Ulnar tuberosity	50	0.097	0.311	0.197	51	0.088	-0.017	0.234
Radial tuberosity	52	0.855	-0.047	0.026	53	0.246	0.059	0.162
Insertion of <i>pronator teres</i>	39	0.101	0.144	0.198	40	0.078	-0.037	0.282
Insertion of <i>supinator</i>	49	0.746	-0.023	0.028	50	0.218	0.017	0.101

*n: number of individuals with paired skeletal elements. p: statistical significance. b; regression coefficient (slope value), r: correlation coefficient

Figure XXI: Regression of the shape values of the AP angle of the radial head and the olecranon.



3.7 Wrist: shape

As shown in Table 15, the posterior ML angle of the distal radius is negatively correlated ($p = 0.032$, $r = 0.253$) with the insertion of the *abductor pollicis longus* (Figure XXII). This result indicates a more keeled angle of the distal radius with stronger muscular contractions, which is contrary to predictions. No other muscle insertion has a significant relationship at the wrist.

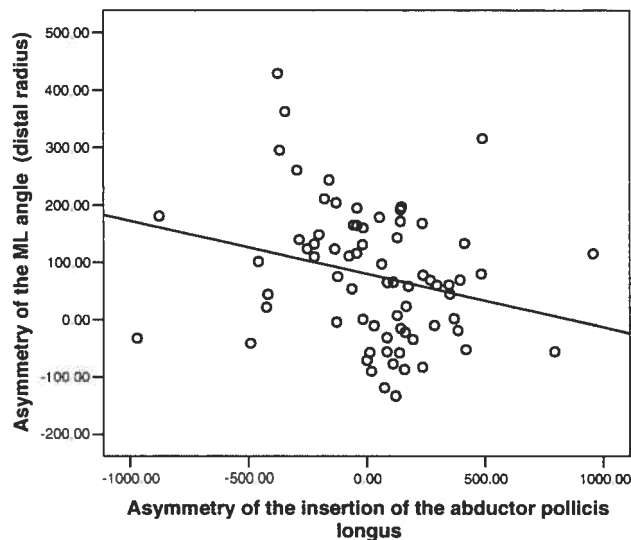
Table 15: Correlation coefficients and significance of the regressions of articular shape and muscle attachment size at the distal radius

Muscle/ Independent variable	ML angle 1				ML angle 2			
	n*	p	b	R	n	p	b	r
Medial epicondyle	74	0.653	-0.017	0.051	75	0.923	-0.007	0.011
Lateral epicondyle	68	0.688	0.007	0.050	68	0.161	-0.153	0.173
Insertion of <i>abductor pollicis longus</i>	71	0.325	0.071	0.119	72	0.032	-0.093	0.253

Muscle/ Independent variable	AP angle 1			
	n	P	b	r
Medial epicondyle	70	0.565	-0.068	0.072
Lateral epicondyle	66	0.696	0.025	0.050
Insertion of <i>abductor pollicis longus</i>	72	0.669	0.043	0.035

*n: number of individuals with paired skeletal elements. p: statistical significance, b: regression coefficient (slope value), r: correlation coefficient

Figure XXII: Regression of the shape values of the ML angle 2 of the distal radius and the insertion of the *abductor pollicis longus* muscle.



3.8 Hand; shape

Finally, Table 16 shows no significant relationships with the muscles crossing the hand joints. Once again, no relation is close to being significant.

Table 16: Correlation coefficients and significance of the regressions of articular shape and muscle attachment size at the hand

Muscle/ Independent variable	Mc1 (SI angle)				Mc1 (ML angle)			
	n*	p	b	R	n	p	b	r
Insertion of <i>abductor pollicis longus</i>	51	0.415	-0.120	0.082	50	0.390	0.077	0.124

Muscle/ Independent variable	Mc3 (SI angle)				Mc3 (ML angle)			
	n	p	b	R	n	p	b	r
Medial epicondyle	56	0.521	0.032	0.117	53	0.669	0.019	0.060
Lateral epicondyle	51	0.260	0.042	0.065	48	0.711	0.008	0.055

*n; number of individuals with paired skeletal elements, p; statistical significance, b; regression coefficient (slope value), r; correlation coefficient

When looking at the shape of the joint in relation to the muscular strength, significant relationships were found only at the elbow and the wrist.

3.9 Summary

Table 17 is a summary of the results of the upper-limb joints in relation to muscular contractions found in this study. The results in this table correspond to the correlations with significance values of $p \leq 0.1$ and correlation coefficients of $r \geq 0.20$. Cohen's paper (1994) shows that significance values can be higher than 0.05, but must be supported by other values, such as the correlation coefficients. Therefore, the discussion that follows this chapter, will investigate the causal effect of the relationships where at least 20% of the variation of the joints size and/or shape can be explained by the muscles crossing them.

Table 17: Summary of the results from the regressions where $p \leq 0.1$ and $r \geq 0.20$.

Articulation	Regression results
Shoulder	Size of humeral head positively correlated with size of greater tubercle
	Size of glenoid surface negatively correlated with size of coracoid process
	SI angle of glenoid surface positively correlated with size of coracoid process
Elbow	Height of capitulum positively correlated with size of lateral epicondyle
	Height of capitulum negatively the size of <i>pronator teres</i>
	Size of humeral trochlea negatively correlated with size olecranon
	Inferior lateral angle of humeral trochlea positively correlated with size of ulnar tuberosity
	Inferior lateral angle of humeral trochlea positively correlated with size of radial tuberosity
	Inferior lateral angle of humeral trochlea positively correlated with size of olecranon
	ML width of inferior portion of proximal ulna articular surface positively correlated with size of olecranon
	Size of the radial notch negatively correlated with size of <i>supinator</i>
	Size of radial head positively correlated with size of radial tuberosity
	Size of radial head negatively correlated with size of medial epicondyle
	AP angle of radial head positively correlated with size of olecranon
	ML angle of radial head positively correlated with size of lateral epicondyle
	ML angle of radial head negatively correlated with lateral size of ulnar tuberosity
	ML angle of radial head negatively correlated with lateral size of <i>pronator teres</i>
Wrist	ML angle of distal radius negatively correlated with size of <i>abductor pollicis longus</i>

Chapter 4: Discussion and conclusion

4.1 General discussion

This project tested the hypothesis that joint surfaces may, in part, be shaped by the mechanical environment. Since most humans use preferably one arm over the other and stronger muscles develop on the preferred side, the main hypothesis of this project was to test whether the side that has larger muscle markings will also have joints that are modelled to accommodate larger loads. For each individual, the joint should be larger and/or of a shape that better resist loads on the preferred side when compared to the other side.

The results of this study have shown little support to the hypothesis stating that the shape and/or size of the articular surfaces will vary according to the different forces that cross the articulations of the upper limbs. No significant relationships were found at the hand. However, a few significant relations were seen at the shoulder, the elbow and the wrist.

4.2 Shoulder

As it was discussed in chapter 1, as the arm rotates at the shoulder articulation, the vector forces push medially the head of the humerus on the scapula (Nordin and Frankel, 2001). It was hypothesized that the articular surface areas of the scapula and the humerus would increase in size to better distribute the larger loads induced by the muscles, and that the glenoid cavity of the scapula would be flatter, meaning an increase in the angles measured (Figure IV). Only three correlations at the shoulder were significant or had a relatively high correlation coefficient. Of the three, two of the results were as hypothesized.

The greater tubercle is the attachment of the *teres minor*, the *supraspinatus* and the *infraspinatus* of the rotator cuff musculature around the shoulder joint. Greater muscle contraction measured at the greater tubercle, seems to result in a larger humeral head.

The glenoid surface is smaller and flatter with greater size of the muscle projection. The coracoid process is the attachment of the *teres minor*, the

coracobrachialis and the *biceps brachii*. These muscles also push medially on the humeral head (Figure IV). Contrary to what was expected the size of the glenoid surface seems to decrease with stronger muscle contractions. However the shape of the glenoid cavity has a supportive correlation, meaning a less concave joint on the favoured side.

These results indicate that the humeral head seems to be greater in size to better resist the loads on the side being most used, but the glenoid cavity on the other hand seems to have a smaller size and a flatter surface. The larger size of the humeral head found here should correspond to an articulation of greater size and of flatter shape, which is partially what, is found at the glenoid cavity. Perhaps the shape of the humeral head might be a more appropriate variable to measure compared to the glenoid surface to detect modelling of the shoulder since the humeral head may be developmentally more plastic than the glenoid cavity on the scapula.

Tanaka (1999) found that the humeral head showed small degree of bilateral size and shape differences and suggested that the overall articular shape changes only slightly with altered mechanical loadings placed on the articular surfaces. His results suggest some plasticity of the joint in response to variation in loads. Like Tanaka, this study found that the humeral head seemed to vary in size to better resist frequent loadings. Further hypotheses on the shape of the humeral head should be tested and the results might also be similar to those found by Tanaka.

4.3 Elbow

Similarly to the shoulder, all of the articulations of the elbow were hypothesized to increase in size in order to better resist the loads. At the distal humerus, greater muscle contractions were theorized to result in an acute angle of the inferior surface of the humeral trochlea with longer medial and lateral trochlear flanges (Figures V and VI). The medial and lateral keels are expected therefore to be longer and more erect to resist the loads generated by the contractions of the muscles that cross the joint obliquely. Finally, the proximal ulnar and radial articular surfaces would be flatter in shape to better resist the

loads produced by the muscle contractions. From the significant relations, a little over half (57%) were as expected.

4.3.1 Distal humerus

Greater muscle contractions on the preferred side seem to result in a greater height of the capitulum. The capitulum correlates positively with the size of the lateral epicondyle, which is the site of attachment of many of the hand and wrist extensors and of supination muscles. This muscle projection was the one variable associated with the highest levels of measurement error (average error of 9.34%). The lateral epicondyle might not therefore be the best indicator of the differential use of the upper limbs. Another method should be used to measure this projection.

Greater height of the capitulum is a similar result to what Plochocki (2004) found. He studied the articular asymmetry to assess the plasticity of limb articular dimension through the use of directional asymmetry as an indicator of mechanical stress during skeletal development. Although Plochocki's methods were different since he only considered articular asymmetry, the height of the capitulum had high statistical significance on the preferred side. Since muscle asymmetry was not a variable like in the present research, Plochoki's significance level was greater than those found here. In general though, the similar results indicate that even though the lateral epicondyle has a high measuring error, the joint at the distal humerus seems to be developmentally plastic to better resist the loads incurred by the muscle contractions.

Be that as it may, the size of the trochlea and the height of the capitulum have a negative correlation with the size of the olecranon and the insertion of the *pronator teres* respectively. These contrary results indicate that the distal articular surface of the humerus is smaller in size with stronger muscular force. The *triceps brachii* muscle, which inserts on the olecranon, generates the largest moment about the elbow joint (An et al., 1981) and is the most powerful muscle of the upper limb (Amis et al., 1979). The *pronator teres* intervenes in the pronation of the radius and aids in the flexion of the elbow (Platzer, 2001;

Marieb, 2000; Tortora and Grabowski, 2001; Slaby et al., 1994). The flexing role of the *pronator teres* opposes the *triceps brachii* muscle and might explain the negative correlation found at the elbow. The *triceps brachii* and the *pronator teres* may act to increase the depth of the trochlea reducing the width in the process. Still, the *triceps brachii* crosses neither laterally nor medially the elbow (An et al., 1981). It is therefore not clear why its contractions would result in a greater depth of the trochlea instead of simply widening it. Plochocki (2004) only looked at the trochlear height but found statistically positive significant correlations associated with the preferred side. The combination of ML and SI measurements of the trochlea might have produced inconclusive results.

Greater angles at the distal humerus are occasionally correlated with larger muscle insertions. The inferior lateral angle of the humerus has a positive relationship with both the ulnar and the radial tuberosities and the olecranon. Both tuberosities are site of powerful flexors of the elbow (*brachialis* and *biceps brachii*), and the olecranon is the site of a powerful extensor (*triceps brachii*). The *brachialis* and the *biceps brachii* generate mostly axial and only little transverse loads with their contractions. Therefore, the lateral lip is not more upright due to the perpendicular loadings (Figure V). Combined action of these flexors with the *triceps brachii* may work together to increase the transverse loads at the joint. The loading effect caused by the muscles at the elbow remains speculative and further work on the muscle loadings needs to be done.

4.3.2 Proximal ulna and radius

The width of the inferior part of the proximal ulna seems to increase with the contractions of the *triceps brachii* which inserts on the olecranon. As expected the strong transverse loadings caused by the pulling of the powerful elbow extensor augments the surface area of the proximal ulna.

The contractions of the *supinator* muscle seem to result in a smaller surface area of the radial notch. Instead of a larger surface area, a greater concavity of the radial notch might be better suited to resist muscle strength.

Yet no articular shape analysis was done for this articular surface. An analysis of the relationship between the shape of the radial notch and the muscle crossing that joint could clarify these results.

The radial head incurs axial loadings generated by the muscles that cross the elbow. The radial head needs to expand on the preferred side to better resist these large loads caused by the contractions of the *biceps brachii*. This result is in agreement with previous work (Plochocki, 2004). However, the opposite result was associated with the medial epicondyle, which is a site of hand and wrist flexor muscles. These muscles generate mostly transverse and not as much axial charges, which might explain why the surface is not reacting in the same way to the contractions of these muscles.

When looking at the shape of the radial head, many interesting results were found. A less concave surface of the radial head seems to be associated with stronger contractions of the muscles that attach to the olecranon and the lateral epicondyle, i.e., the radial head appears to be flatter to better resist the loads of the muscle contractions caused by extensor muscles. So, loads caused by muscle strength push the ulna and radius on the humerus. The surface of the radial head will tend to flatten to better resist these loads.

On the other hand, the concavity of the radial head seems to increase with the powerful actions of the *pronator teres* and the *brachialis*, i.e., the joint becomes more concave with greater muscle contractions. Strong flexors of the elbow do not tend to flatten the radial head as was predicted, but tend to increase the size of the articular surface and the concavity instead. Therefore, at the elbow, greater flexing forces may result in a greater surface area but a deeper concavity of the radial head. Both the insertions of the *pronator teres* and the *brachialis* have been associated with results opposing the predictions. These muscle markings may not be good indicators of the differential use of the upper limbs. They may not be the best insertions to be used as surrogate for muscular strength. Having a higher sample size may also infirm or confirm these results.

4.4 Wrist

Finally, at the wrist, flatter and larger articular surfaces were expected to better distribute the greater loads induced by muscle contractions. The *abductor pollicis longus* muscle serves as the abductor and an extensor for the thumb but also as an abductor of the hand the wrist. Contrary to what was expected, the surface area of the distal radius is more concave with greater abducting forces passing through the joint. Perhaps pulls from the *abductor pollicis longus* at the wrist may tend to dislocate the radius. The disto-medial end of the radius may need to be more erect to better resist the pulling of the abducting muscle. This interpretation remains highly speculative. In a previous study done by Plochocki (2004), the distal radius also gave inconclusive results.

4.5 Conclusion

After taking a look at these results, it should not be forgotten that a very small percentage of the analyses performed produced significant results. Possibly, the differences in the right-left articulations may be very small. The sample size of 108 individuals was in fact ranging from 32 to 87 individuals depending on the analysis. These numbers might be too small to observe any significant differences in these upper-limb joints. Further work with an enlarged sample may help resolve this issue.

In general, at each articulation, it was expected to see articulation that are generally larger on the preferred side and that may have a different form, which was usually predicted to be flatter. After doing these analyses, it is clear that some changes are expected at the articulations with stronger muscle contractions. It would be interesting to investigate further to see how exactly the articulations are modified due to greater loadings created by the contractions of the surrounding muscles. Increasing the number of individuals in the sample and doing an accurate three-dimensional analysis of the articulations used in this study might increase the possibility of a better understanding of how joints are modified during growth by muscular contractions. Although there is little evidence that the upper-limb articulations

are asymmetrical relative to the muscular asymmetry, there were a few significant correlations that indicated a change in size and/or shape of the articulation, whether the correlation was in the direction predicted or not. An important next step would be to investigate articulations during development in humans, in order to have a better perspective of how joints are modelled during growth.

Other very important points have to be considered. As discussed by Auerbach and Ruff (2006), the articulations may not be as plastic in humans as they have been found to be in animals (Frost, 1999; Hamrick, 1999b; Carter and Beaupré, 2001; Plochocki, 2006). Auerbach and Ruff (2006) also found that relative to other measures (diaphyseal breadth, length and articular dimensions) articular dimensions in humans always seem to exhibit the least asymmetry. More work is needed to clarify if mechanical loading can influence chondral and subchondral tissue proliferation to provide greater support against increasing mechanical loadings in humans as it seems to do in animals (Plochocki, 2006).

Muscle markers were used as a surrogate for muscular strength to determine whether articulations could show similar asymmetry. The method used to measure muscle attachments may not have been a good indicator of the muscular strength. Like Wilczak (1998a, b) a relatively high percentage of measurement error was found using this quantitative method. In addition, as was mentioned in chapter 2, since bone is a three-dimensional structure, information about the morphology of the insertion site is lost by measuring the maximum length and width and rugosity is not considered. Perhaps using a combination of the quantitative (Wilczak, 1998a, b) and qualitative methods (Hawkey and Merbs, 1995) would increase the chance of capturing better the representation of the muscular strength exhibited by the muscle contractions.

Alternatively, the lack of differences might be due to the fact that muscular development occurs fairly late in the growth process, possibly after articulations have already completed their formation and are much less plastic than they are during growth. Also, as discussed by Zumwalt (2005) muscle

insertions are possibly not the best evaluators of the muscular strength. Muscle attachments in this study may not have been the best indicators of the differential use of the upper limbs. Despite a differential use of the upper limbs, the loads may actually not be as different as it was assumed. Further work needs to be done to better comprehend the differential loadings of the contraction of the muscles on the articulations, particularly in the upper limbs.

Finally, the lack in differences between the upper limbs may be due to the heterogeneity of the sample. Diverse geographic origins found in the sample as well as the lack of distinction between the sexes and the ages of the individuals might have covered some of the relationship between the articular surfaces and the muscle attachments. A general phenomenon was investigated by combining many different aspects into the sample. Despite the debates on the effects of age difference, separation of the sexes and the different geographic locations (Hawkey and Merbs, 1995; Wilczak, 1998a, b; Eshed et al., 2003; Ruff, 2003; Weiss, 2003, 2004; Zumwalt, 2005; Molnar, 2006), taking a closer look at the different groups could have shed some light on how muscle strength can have influence the joints size and/or shape. Therefore, the next step would be to study joint architecture and muscle markers variation within a single population to reconstruct the activity patterns of the individuals in the groups

In conclusion, this research found that there is little evidence that upper-limb articulations are asymmetrical relative to muscular asymmetry. The hypothesis stating that the side with larger muscle markings will have joints that are larger and/or have a different shape is only supported by a few significant comparisons. A few relationships have regression coefficients that are close to be statistically significant ($p \leq 0.1$). This suggests that differences in the articulations may be very small and the sample not large enough to observe any significant differences in the upper-limb joints. A sample with more individuals could help bring in more statistical significance to these tests.

Future research on this subject needs to explore in more details the development of the articulations and the muscle insertions in order to better

understand how the mechanical environment could be affecting the formation of the articulations. This project does show that there is plasticity in the articulations of the upper-limb joints of humans. Further work looking at the differences in age, sex, geographic origins, various activities and pathologies need to be accomplished to have a better understanding of the articular responses to mechanical stress. Yet, this study brought questioning in the use of muscular attachments to be used as surrogate of muscle strength. Further investigations needs to be done to fully comprehend the relationship between the muscles and their corresponding markings on the bones.

Bibliography

Agarwal, S.C. and S.D. Stout. 2003. *Bone loss and osteoporosis: an anthropological perspective*. Kluwer Academic/Plenum Publishers, New York.

Aiello, L. and C. Dean. 1990. *An introduction to Human evolutionary anatomy*. Academy Press, London.

Auerbach, B.M. and C.B. Ruff. 2004. *Human body mass estimation: a comparison of "morphometric" and "mechanical" methods*. American Journal of Physical Anthropology, 125: 331-342.

Auerbach, B.M. and C.B. Ruff. 2006. *Limb bone bilateral asymmetry: variability and commonality among modern humans*. Journal of Human Evolution, 50: 203-218.

Allard, P. et J-P. Blanchi. 2000. *Analyse du mouvement humain par la biomécanique*. Deuxième édition. Décarie Éditeur Inc., Mont-Royal, Québec.

Amis, A.A. D. Dowson and V. Wright. 1979. *Muscle strengths and musculo-skeletal geometry of the upper limb*. Engineering Medicine, 8.1: 41-48.

Amis, A.A., D. Dowson and V. Wright. 1980. *Elbow joint force predictions for some strenuous isometric actions*. Journal of Biomechanics, 13: 765-775.

An, K.S., F.C. Hui, D.F. Morrey, R.L. Linscheid and E.Y. Chao. 1981. *Muscles across the elbow joint: a biomechanical analysis*. Journal of Biomechanics, 14: 659-669.

Ankel-Simons, F. 2000. *Primate anatomy: an introduction*. Second Edition. Academic Press, San Diego, California.

Bertram, J.E.A. and S.M. Swartz. 1991. *The "law of bone transformation": a case of crying Wolff?* Biology Review, 66: 245-273.

Buikstra, J.E and D.H. Ubelaker. 1994. *Standards for data collection for human skeletal remains*. Arkansas archeological survey, Fayetteville, Arkansas.

Carter D.S. and G.S. Beaupré. 2001. *Skeletal function and form: mechanobiology of skeletal development, aging and regeneration*. Cambridge University Press, Cambridge.

Cohen, J. 1994. *The earth is round ($p < .05$)*. American Psychologist, 49: 997-1003.

Currey, J. 1984. *The mechanical adaptations of bones*. Princeton University Press, New Jersey.

DeLisa, J. and W.C. Stolove. 1981. *Significant body systems, in: handbook of severe disability*. Edited by Walter C. Stolov and Michael R. Clowers. US Department of Education, Rehabilitation Services Administration.

Demes, B., J.T. Stern Jr., M.R. Hausman, S.G. Larson, K.J. Mcleod and C.T. Rubin. 1998. *Patterns of strain in the macaque ulna during functional activity*. American Journal of Physical Anthropology, 106: 87-100.

DePuy Orthopaedics Inc. 2000-2005. *All about arthritis*, Johnson Johnson company, Online; <http://depuyorthopaedics.com>.

Drapeau, M.S.M., 2004. *Functional anatomy of the olecranon process in Hominoids and Plio-Pleistocene Hominins*. American Journal of Physical Anthropology, 124: 297-314.

Eshed, V., A. Gopher, E. Galili and I. Hershkovitz. 2004. *Musculoskeletal stress markers in Natufian hunter-gatherers and Neolithic farmers in the Levant: The upper limb*. American Journal of Physical Anthropology, 123: 303-315.

Freivalds, A. 2004. *Biomechanics of the upper limbs: mechanics, modeling and musculoskeletal injuries*. CRC Press, Florida.

Frost, H.M. 1990a. *Skeletal structural adaptation to mechanical usage (SATMU): 1. Redefining Wolff's Law: the bone modeling problem*. The Anatomical Record, 226: 403-413.

Frost, H.M. 1990b. *Skeletal structural adaptation to mechanical usage (SATMU): 2. Redefining Wolff's Law: the bone remodeling problem*. The Anatomical Record, 226: 414-422.

Frost, H.M. 1994. *Perspectives: a vital biomechanical model of synovial joint design*. The Anatomical Record, 240: 1-18.

Frost, H.M. 1999. *Joint anatomy, design, and arthroses: insights of the Utah paradigm*. The Anatomical Record, 255: 162-174.

Gunn, C. 1984. *Bones and joints; a guide for students*. Churchill Livingstone, New York.

Hamrick, M.W. 1999a. *Development of epiphyseal structure and function in Didelphis virginiana (Marsupiala, Didelphidae)*. Journal of Morphology, 239: 283-296.

- Hamrick, M.W. 1999b. *A chondral modeling theory revisited*. Journal of Theoretical Biology, 201: 201-208.
- Hamrick, M.W., A.C. McPherron, C.O. Lovejoy and J. Hudson. 2000. *Femoral morphology and cross-sectional geometry of adult myostatin-deficient mice*. Bone, 27: 343-349.
- Hawkey, D.E. and C.F. Merbs. 1995. *Activity induced musculoskeletal stress markers (MSM) and subsistence strategy changes among ancient Hudson Bay Eskimos*. International Journal of Osteoarchaeology, 5: 324-338.
- Hawkey, D.E. 1998. *Disability and skeletal record: using musculoskeletal stress markers (MSM) to construct an osteobiography from Early New Mexico*. International Journal of Osteoarchaeology, 8: 326-340.
- Hildebrand, M. 1988. *Analysis of vertebrate structure*. John Wiley & Sons Inc., New York.
- Holliday, T.W. and C.B. Ruff. 2001. *Relative variation in Human proximal and distal limb segment lengths*. American Journal of Physical Anthropology, 116:26-33.
- Knusel, C. 2000. Bone adaptation and its relationship to physical activity in the past. In *Human osteology in archeology and forensic science*. Edited by M. Cox and S. Mays, Greenwich Medical Media Ltd., London, pages 381-402.
- Li, G., J.E. Pierce and J.H. Herndon. 2006. *A global optimization method for prediction of muscle forces of human musculoskeletal system*. Journal of Biomechanics, 39: 522-529.
- Lieberman, D. E. and A.W. Crompton. 1998. Responses of bone to stress: constraints on symmorphosis. In *Principles of animal design: the optimization and symmorphosis debate*. Edited by E.R. Weibel, C.R. Taylor and L. Bolis, Cambridge University Press, Cambridge.
- Lieberman, D.E., M.J. Devlin and O.M. Pearson. 2001. *Articular area response to mechanical loading: effects of exercise, age, and skeletal location*. American Journal of Physical Anthropology, 116: 266-277.
- Lieberman, D.E., J.D. Polk, and B. Demes. 2004. *Predicting long bone loading from cross-sectional geometry*. American Journal of Physical Anthropology, 123: 156-171.
- Marieb, E.N. 2000. *Essentials of human anatomy and physiology*. Sixth Edition. Addison Wesley Longman Inc., San Francisco.

Martin, R. and K. Saller. 1957. *Lehrbuch der anthropologie*. Gustav Fischer Verlag, Stuttgart.

Martin, B.R., D.B Burr and N.A. Sharkey 1998. *Skeletal tissue mechanics*, Springer-Verlag, New York.

Martin, B.R. 2000. *Toward a unifying theory of bone remodelling*. Bone, 26: 1-6.

Mays S., J. Steele and M. Ford. 1999. *Directional asymmetry in the human clavicle*. International Journal of Osteoarchaeology, 9:18-28.

Molnar, P. 2006. *Tracing Prehistoric activities: musculoskeletal stress marker analysis of a Stone-Age population on the Island of Gotland in the Baltic Sea*. American Journal of Physical Anthropology, 129: 12-23.

Nijhof, E.J. and D.A. Gabriel. 2006. *Maximum isometric arm forces in the horizontal plane*. Journal of Biomechanics, 39: 718-716.

Nordin, M. and V.H. Frankel. 2001. *Basic biomechanics of the musculoskeletal system*. Third Edition. Lippincott Williams & Wilkins, Philadelphia.

Pauwel, F. 1980. *Biomechanics of the locomotor apparatus; contributions on the functional anatomy of the locomotor apparatus*. Springer-Verlag, Berlin.

Pearson, O.M. and D.E. Lieberman. 2004. *The aging of Wolff's law: ontogeny and responses to mechanical loading in cortical bone*. Yearbook of Physical Anthropology, 47: 63-99.

Pierce, J.E. and G. Li. 2005. *Muscle forces predicted using optimization methods are coordinate system dependent*. Journal of Biomechanics, 38: 695-702.

Platzer, W. 2001. *Atlas de poche d'anatomie; appareil locomoteur*. Troisième édition. Médecine Sciences Flammarion, Paris.

Plochocki, J.H. 2002. *Directional bilateral asymmetry in human sacral morphology*. International Journal of Osteoarchaeology, 109:457-459.

Plochocki, J.H. 2003. *Mechanical regulation of limb joint growth: computational analysis of chondral modeling and implications for the reconstruction of behaviour from articular form*. Ph.D. dissertation, University of Missouri, Columbia, MO.

Plochocki, J.H. 2004. *Bilateral variation in limb articular surface dimensions*. American Journal of Human Biology, 16: 328-333.

- Plochocki, J.H. et al. 2006. *Functional adaptation of the femoral head to voluntary exercise*. The Anatomical Record Part A, 288A: 776-781.
- Rose, M.D. 1988. *Another look at the anthropoid elbow*. Journal of Human Evolution, 17: 193-224.
- Rose, M.D. 1993. Functional anatomy of the elbow and forearm in primates. In *Postcranial adaptation in nonhuman primates*, Ed. D.L. Gebo, Northern Illinois University Press, Dekalb, pages 70-95.
- Ruff, C.B. and W.C. Hayes. 1983. *Cross-sectional geometry of Pecos Pueblo femora and tibiae – a biomechanical investigation: I. Method and general patterns of variation*. American Journal of Physical Anthropology, 60: 359-381.
- Ruff, C.B. et al., 1997. *Body mass encephalization in Pleistocene Homo*. Nature, 387: 173-176.
- Ruff, C.B. 2000. Biomechanical analyses of archeological Human skeletons. In *Biological Anthropology of the Human skeleton*. Edited M. A. Katzenberg and S.R. Saunders. John Wiley and Sons Inc., Toronto, pages 71-102.
- Ruff, C.B. 2002a. *Long bone articular and diaphyseal structure in Old World Monkeys and Apes. 1: locomotor effects*. American Journal of Physical Anthropology, 119: 305-342.
- Ruff, C.B. 2002b. *Variation in human body size and shape*. Annual Review in Anthropology, 31: 211-232.
- Ruff, C.B. 2003. *Growth in bone strength, body size, and muscle size in a juvenile longitudinal sample*. Bone, 33: 317-329.
- Ruff, C.B. 2005. *Growth tracking of femoral and humeral strength from infancy through late adolescence*. Acta Paediatrica, 94: 1030-1037.
- Saunders, S.R. 2000 Subadult skeletons and growth-related studies. In *Biological anthropology of the Human skeleton*. Edited by M.A. Katzenberg and S.R. Saunders. John Wiley and Sons Inc., Toronto, pages 135-162.
- Scherrer, B. 1984. *Biostatistique*. Gaetan Morin Éditeur ltée., Boucherville, Québec.
- Scheuer, L. and S. Black. 2000. *Developmental juvenile osteology*. Elsevier Academic Press, London.

Schmitt, D. 2003. *Mediolateral reaction forces and forelimb anatomy in quadrupedal primates: implications for interpreting locomotor behaviour in fossil primates*. *Journal of Human Evolution*, 44: 47-58.

Sénécal, C. 2003. *Cours de musculation*. Collège Édouard-Montpetit, Online; <http://ww2.college-em.qc.ca>.

Slaby, F.J., R. Summers and S. McCune. 1994. *Gross Anatomy in the practice of medicine*. Lea & Febiger, Philadelphia.

SPSS 13.0 for Windows. 2004.

Steele, J. and S. Mays. 1995. *Handedness and direction asymmetry in the long bones of the human upper limb*. *International Journal of Osteoarchaeology*, 5:39-49.

Steele, J.. 2000 Skeletal indicators of handedness. In *Human osteology in archeology and forensic science*. Edited by M .Cox and S. Mays, Greenwich Medical Media Ltd., London, pages 307-324.

Stock, J. & S. Pfeiffer. 2001. *Linking structural variability in long bone diaphyses to habitual behaviors: foragers from the Southern African Later Stone Age and the Andaman Islands*. *American Journal of Physical Anthropology*, 115:337-348.

Swartz, S.M. 1993. Biomechanics of primate limbs. In *Postcranial adaptation in nonhuman primates*. Edited by D.L. Gebo. Northern Illinois University Press, Dekalb, pages 5-42.

Takakura, Y., S. Tamai and K. Masuhara. 1986. *Genesis of the ball-and-socket ankle*. *The Journal of Bone and Joint Surgery*, 68: 834-837.

Tanaka, H. 1999. *Numerical analysis of the proximal humeral outline: bilateral shape differences*. *American Journal of Human Biology*, 11: 343-357.

Tortora, G.J. et S.R. Grabowski. 2001. *Principe d'anatomie et de physiologie*. Éditions du Renouveau Pédagogique Inc. Saint-Laurent, Québec.

Turner, C.H. 1998. *Three rules for bone adaptation to mechanical stimuli*. *Bone*, 23: 399-407.

Weiss, E. 2003. *Understanding muscle markers: aggregation and construct validity*. *American Journal of physical Anthropology*, 121: 230-240.

Weiss, E. 2004. *Understanding muscle markers: lower limbs*. *American Journal of Physical Anthropology*, 125: 232-238.

White, T.D. and P.A. Folkens. 2001. *Human osteology*. Elsevier Academic Press, London.

White, T.D. and P.A. Folkens. 2005. *The human bone manual*. Elsevier Academic Press, London.

Wilczak, C. 1998a. *Consideration of sexual dimorphism, age and asymmetry in quantitative measurements of muscle insertion site*. International Journal of Osteoarcheology, 8:311-325.

Wilczak, C. 1998b. *A new method for quantifying musculoskeletal stress markers (MSM): a test of the relationship between enthesis size and habitual activity in archeological populations*. Ph.D. dissertation, Cornell University, Ithaca, New York.

Woo, S.L., S.C. Kuei, D. Amiel, M.A. Gomez, W.C. Hayes, F.C. White and W.H. Akeson. 1981. *The effect of prolonged physical training on the properties of long bone: a study of Wolff's law*. The Journal of Bone and Joint Surgery, 63A: 780-787.

Zumwalt, A.C. 2005. *The effect of endurance exercise on the morphology of muscle attachment sites: an experimental study in sheep (Ovis aries)*. Ph.D. dissertation, Johns Hopkins University, Baltimore, Mariland.

